Identifying the protein interactions of Mre11-Rad50 in *Haloferax volcanii* during double-strand break repair

Charlie Wickham-Smith, BSc.

Thesis submitted to the University of Nottingham for the degree of Master of Research

September 2015

Contents

Abstract

The Mre11 and Rad50 proteins are found in all domains of life and form a complex that locates and binds to DNA double-strand breaks (DSBs). The complex tethers DNA ends and coordinates the repair of DSBs. In *Haloferax volcanii, mre11rad50* mutants are more resistant to DNA damage than the wild-type. Mre11-Rad50 is believed to restrain repair of DSBs by homologous recombination (HR) while other repair pathways can operate. Mutants of *mre11rad50* cannot utilise this restraining mechanism so HR is believed to solely repair DSBs, leading to an increase in DNA damage resistance. *H. volcanii* is highly polyploid, possessing up to 20 copies of its genome. This restraining method of repair will prevent DNA ends engaging with multiple partners, which could be highly toxic. The specific details of how *H. volcanii* repair DSBs are unknown, including the protein interaction of Mre11-Rad50.

Mre11-Rad50 has been labelled with His_6 and StrepII tags then purified on gravity columns. Several proteins have been shown to co-purify with His_6/StrepII-tagged Mre11-Rad50 under normal growth conditions. To discover whether these proteins are present during DSB repair, protein purification following incubation with DNA damaging agents is required. Further analysis of these proteins will reveal their identity and whether they are playing a role in DSB repair in *H. volcanii*

Acknowledgements

I would like to sincerely thank Thorsten for giving me the opportunity to carry out research in his lab, also for his patience and advice throughout my MRes. The project has been challenging but thoroughly interesting and I have learned a great deal in the past year.

Thanks to Hannah and Becca for all their help and support and for making each day in the lab so enjoyable.

Thanks to Laura and Jaime for their tireless effort to make the Allers lab run so smoothly and to the Bolt lab for the interesting talks during lab meetings. It was genuinely inspiring to see new ideas being discussed at the forefront of this field.

Special thanks to my family and friends who have supported me and kept me going over the past year.

Chapter 1: Introduction

1.1 Archaea

Until recently Archaea was not recognised as a major Domain of life and the prokaryotic organisms within it were originally thought to be bacteria due to their shared morphological features; lacking membrane-bound organelles and nuclei. It was not until Carl Woese phylogenetically mapped the small subunit of ribosomal RNA (16S rRNA) (Fig. 1.1) that the three-domain classification of organisms was established (Eukaryotes, Bacteria and Archaea) (Woese 1977, Winker 1991). The high level of sequence conservation in this essential component enabled Woese to perform fine-scale phylogenetic analysis on individual base substitutions.

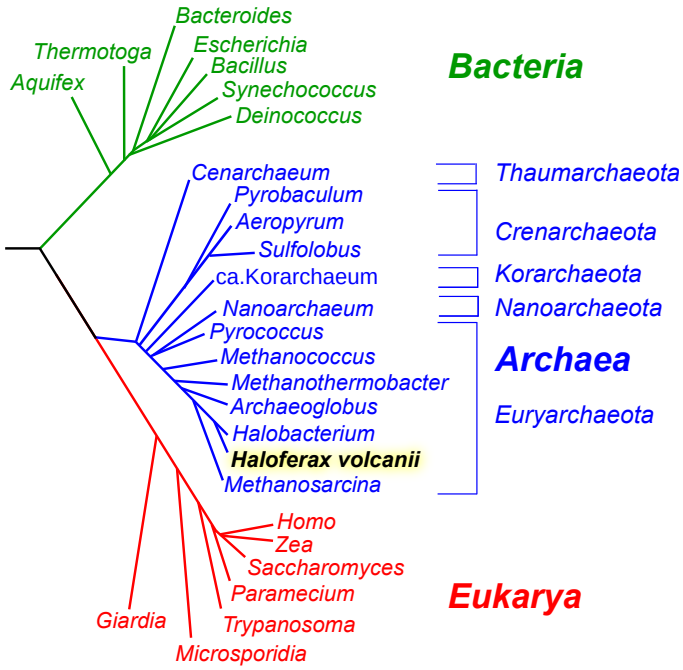

Figure 1.1: **Phylogenetic tree derived from 16S rRNA sequencing**. Bacteria, Archaea and Eukaryotes represent the 3 domains of life. Adapted from Allers & Mevarech (2005)

There are a number of different archaeal phyla that have recently been identified; the Thaumarcheaota (Brochier-Armanet 2008), the Nanoarcheaota (Hohn 2002), the Korarcheaota (Auchting 2006) and the Aigarchaeota (Nunoura *et al.* 2011). The most

extensively studied phyla are Euryarchaeota and the Crenarcheota (Winker 1991, Woese 1990), although currently only 100 archaeal genome have been published (Brochier-Armanet 2011). Recent findings have proposed a two-domain classification with just Bacteria and Archaea (Raymann *et al.* 2015), where eukaryotes are thought to be a sub-domain of Archaea, emerging from Thaumarcheaota/ Aigarchaeota/ Crenarchaeota/ Korachaeota (TACK).

Archaea share many integral features of their DNA processing machinery with eukaryotes such as DNA replication and repair enzymes (Allers & Mevarech 2005). This includes the Mre11Rad50 complex (SbcCD in Bacteria), which is conserved across all domains of life and is involved in multiple pathways of DSB repair. The role of this protein complex will be discussed in more detail.

Halophiles

Salt lakes, acid pools and hydrothermal vents are some of the extreme environments which archaea inhabit. Halophiles exist in high salt environments so must constantly maintain an osmotic balance between intracellular and extracellular salt concentrations. They achieve this by using two alternative strategies. The 'salt out' strategy, adopted by many halophilic bacteria and eukaryotes allows a low intracellular salt concentration to be retained (Christian and Waltho 1962). Organic osmotic solutes are accumulated in the cytoplasm whilst ions are actively pumped out of the cell to maintain osmostasis (Oren 1999). Alternatively osmotic equilibrium is maintained using the 'salt-in' strategy where potassium ions are primarily accumulated to maintain high levels of intracellular salt. Organisms adopting this strategy possess specially adapted proteins that are able to function in such conditions where water availability is low.

Haloferax volcanii

The halophilic euryarchaeon *Haloferax volcanii* was first discovered in the Dead Sea (Mullakhanbhai 1975) and preferentially grow in 1.5-2.5M salt at 45˚C with a generation time of 2.5-3 hours. *H. volcanii* cells possess a glycoprotein surface (S)-layer (Sleytr 1983) and tend to be coccoid. There are multiple genetic tools that have

been developed for this species of archaea, which can also be cultured easily making them an ideal model organism for genetic studies.

H.volcanii have been shown to be naturally polyploid, with up to 20 copies of its genome during exponential phase (Breuert et al. 2006). The chromosome of *H. volcanii* is ~4.2 Mb and consists of one main circular chromosome (2.9 Mb) and four megaplasmids: pHV1 (86 Kb), pHV3 (442 Kb), pHV4 (690 Kb) and wild-isolates also possess pHV2 (6 Kb). The laboratory strain used in this study has pHV4 integrated on the main chromosome but is missing pHV2 (Hawkins *et al.* 2013).

1.2. DNA Repair

1.2.1. DNA Damage

DNA is continuously subject to damage by both endogenous and exogenous sources and must be repaired to prevent the occurrence of harmful mutations. Endogenous damage is consequence of normal metabolic processes such as the production of reactive oxygen species or mistakes made during DNA replication. These processes can cause bases to become damaged. This can cause DNA polymerase to mis-read bases, incorporating incorrect nucleotides during DNA replication. As DNA polymerases are unable to detect misincorporated bases this can be particularly detrimental. DNA damage through exogenous sources can arise through irradiation or chemical mutagens and can be highly cytotoxic.

Exogenous Damage

Ultraviolet light can be absorbed by double bonds between pyrimidine bases, causing various lesions in DNA (Sinha and Hader 2002). The bond will open and may react with a neighbouring pyrimidine causing a cyclobutane pyrimidine dimer (CPD) or a (6-4) photoproduct. Upon acquiring these lesions the DNA backbone becomes distorted, causing them to become ‘bulky’. If these lesions are not repaired, bases can be misincorporated during DNA replication, which will stall a DNA replication fork and form a single or double-strand break (DSB). UV-irradiation also can indirectly cause a DSB if two single strand breaks occur in close proximity (Lankinen et al. 1996).

1.2.2 Double-Strand Break Repair

Programmed DSBs occur as a key step during meiosis in eukaryotes and are generated during V(D)J recombination in vertebrates, an essential stage of immune system development (Bassing et al. 2002; Keeney 2008). However DSBs are highly toxic if left unrepaired and can lead to genome rearrangements or cell death. These lesions can be repaired by either non-homologous end-joining (NHEJ) or micro-homology mediated end-joining (MMEJ). Both involve the processing and re-ligating of DNA ends but are potentially mutagenic and can result in the occurrence of deletions. Alternatively homologous recombination (HR) can also be used to repair DSBs. Although this mechanism is slower, it is far more accurate because an undamaged homologous DNA sequence is used as a template for repair. However genome rearrangements may occur if this repair pathway if left to function unrestrained.

Non-homologous end-joining

Eukaryotic cells primarily use NHEJ to repair DSBs during G1 phase (Lieber 2010) but only certain bacteria and archaea use this repair pathway. Neither *H. volcanii* nor *E. coli* adopt this mechanism (Brisset and Doherty 2009; Bowater and Doherty 2006). NHEJ in bacteria and eukaryotes requires Ku (Ku70/80 in eukaryotes); an enzyme that binds to DNA ends and forms a scaffold around dsDNA for other repair enzymes (Walker et al. 2001; Lieber 2010). LigD is used in bacteria (Weller and Doherty 2001) and possesses polymerase, exonuclease and ligase domains. This multifunctional enzyme processes DNA ends by either filling in or resecting overhangs and ligating the ends. Multiple enzymes alternatively carry out end processing in eukaryotes. DNA polymerases λ and μ are used to fill in, the exonulease Artemis resects and the XLF:XRCC4:ligIV complex carries out ligation.

Microhomology mediated end-joining

MMEJ has been studied less extensively in comparison to NHEJ and HR but is a common method of DSB repair seen in eukaryotes, archaea and some bacteria (McVey & Lee 2008). Eukaryotes use the Mre11 complex to promote MMEJ, which degrades DNA overhangs until short regions of homology are identified (Ma et al. 2003; Paul and Gellert 2000) (Fig. 1.2). 3’ flaps of non-complementary regions form

when the regions of microhomology anneal and are removed by Rad1-Rad10 endonuclease. This method is error prone due to the deletions that occur when the gaps are filled prior to ligation (Ma et al. 2003; McVey and Lee 2008).

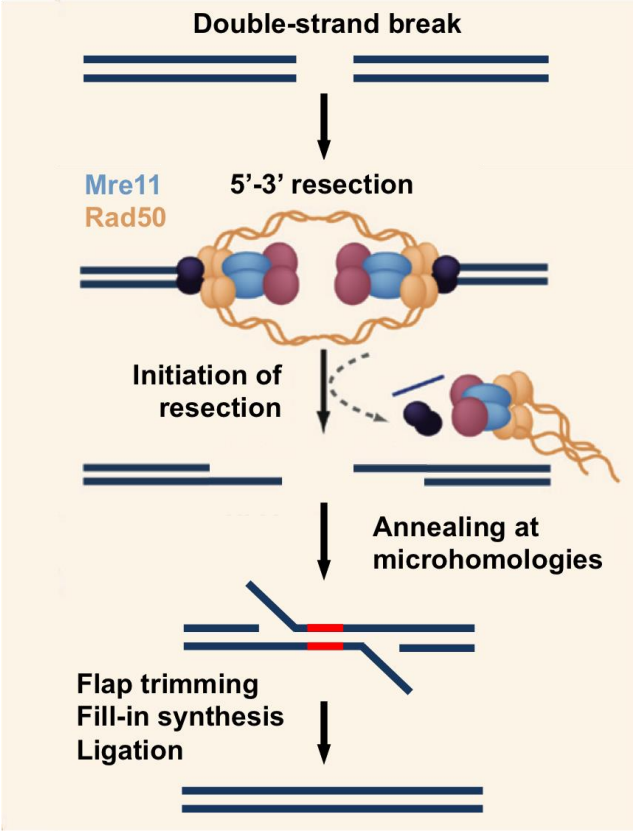

Figure 1.2: **Microhomology-mediated end joining (MMEJ).** DSB is sensed by Mre11-Rad50, which carries out limited end resection (5'-3'). Regions of microhomology anneal. Flaps are cleaved, gaps filled and ligated. (Adapted from Mazón *et al.* 2010)

Homologous Recombination

DSBs can be repaired by HR, a highly accurate method of repair that uses an intact homologous DNA molecule as a template. The conserved mechanism of HR can be broken down into three broad steps: pre-synapsis, synapsis and post-synapsis.

Pre-synapsis

Pre-synapsis involves 5'-3' resection of DSBs to produce 3' ssDNA overhangs. Initial resection of DNA ends is carried out by Mre11-Rad50 in eukaryotes and archaea (Trujillo *et al.* 1998; Usui *et al.* 1998; Hopkins & Paull 2008). The endonuclease activity of Sae2/CtIP is stimulated by Mre11-Rad50 in eukaryotes to generate a

minimally resected intermediate (Lengsfeld *et al.* 2007). Extensive end resection is then carried out by the 5'-3' exonuclease ExoI. The intermediate may be alternatively processed by the helicase SgsI/BLM, which is thought to operate in conjunction with Dna2 exonuclease to carry out extensive end resection (Mimitou & Symington 2008; Blackwood *et al.* 2013). The combined helicase and nuclease activity of the RecBCD complex processes DSBs (including RecA loading) in gram-negative bacteria such as *E. coli* (Wigley 2013). Archaea lack homologs of these bacterial and eukaryotic enzymes (Blackwood *et al.* 2013), however thermophilic archaea possess NurA (5'-3' exonuclease) and the helicase HerA, which resect DSBs (Blackwood *et al.* 2012).

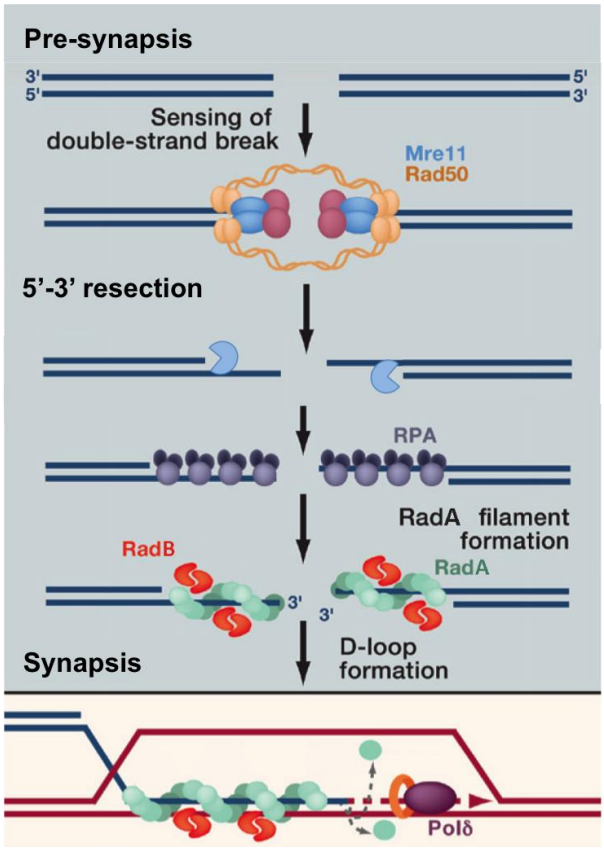

Figure 1.3: **Pre-synapsis & Synapsis of homologous recombination in *H. volcanii*.** Mre11-Rad50 senses a DSB and begins end resection. Extensive resection carried out by unknown enzymes and RPA loaded onto 3' strand. RadB acts as a recombination mediator for RadA. 3' strand loaded with RadA carries out strand invasion of intact duplex DNA, forming a D-Loop. (Adapted from Mazón *et al.* 2010)

3' ssDNA overhangs are coated with single stranded binding protein (SSB/RPA) to protect the strand from degradation. Recombination mediators displace SSB/RPA and assist the loading of recombinases onto 3' ssDNA to form a nucleoprotein filament.

Bacteria use the RecFOR complex to displace SSB and assist the loading of RecA onto ssDNA or can be used if RecBCD is not present to process DSBs (Sakai & Cox 2009). Eukaryotes possess a range of recombination mediators including Rad52, Swi5-Srf2, Rad54, Rad55-Rad57 (yeast), XRCC2, XRCC3, Rad51B, Rad51C and Rad51D (vertebrates) and BRCA2 (mammals). These aid in the formation of Rad51 nucleoprotein filaments (Sugiyama and Kowalczykowski 2002; Kuwabara et al. 2012; Mazin et al. 2003; Sung 1997; Sigurdsson et al. 2001; Lio et al. 2003; Holthausen et al. 2011; Liu et al. 2010). Euryarchaea possess RadB, which may assist the loading of RadA (Haldenby 2007) (Fig. 1.3). *S. solfotaricus* possess SsoRal1, which could function as a recombination mediator for RadA but may function as an anti-recombinase (Graham *et al.* 2013; McRobbie *et al.* 2009). Anti-recombinases can disassemble nucleoprotein filaments and restrain recombination such as Srs2 found in yeast (Krejci *et al.* 2012).

Synapsis

During synapsis, the nucleoprotein filament engages dsDNA and carries out a homology search. The single-strand invades the double-stranded duplex at regions of homology (strand exchange). This forms a joint molecule known as a D-loop (displacement loop).

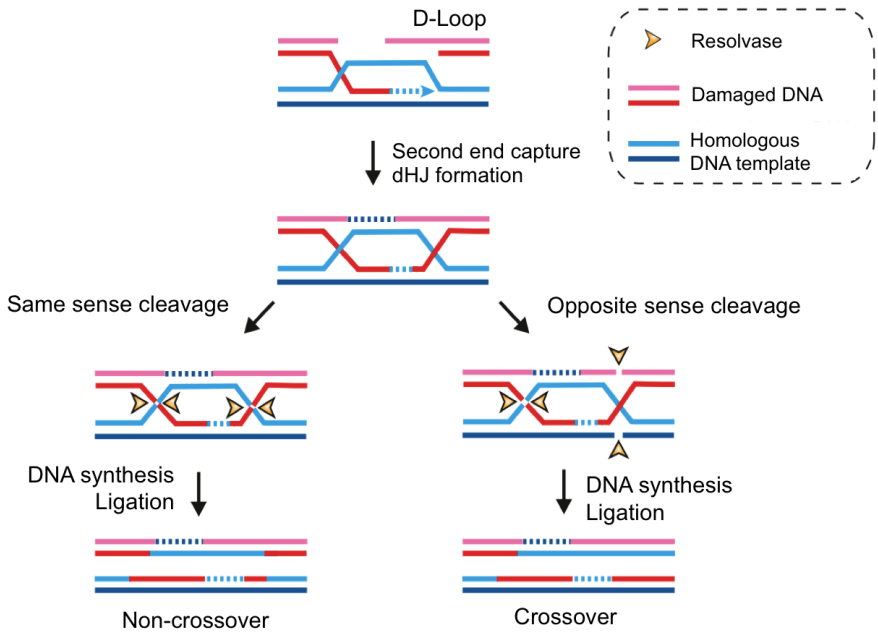

Figure 1.4: **Post-synapsis: Resolution of double Holliday junction.** Non-crossover recombination event results from same sense cleavage by resolvases. Crossover recombination event results from opposite sense cleavage. (Wardell 2013).

Post-synapsis

Post-synapsis involves the processing and subsequent repair of the joint molecule, which requires second end capture and double-Holliday junction formation. Holliday junctions are mobile junctions formed between two duplexes and must be processed to separate the two DNA molecules. Resolvases act on branched DNA-structures and cleave double Holliday junctions either in the same, or opposite orientations. This produces a crossover or a non-crossover recombination event (Fig. 1.4).

Bacteria utilise the RuvABC complex for Holliday junction migration and cleavage (West 2003). RuvA and RuvB promote branch migration whilst the endonuclease RuvC binds to the junctions as a dimer, cleaving the junction by dual symmetric incision. Eukaryotes possess multiple pathways of Holliday junction resolution (Schwartz and Heyer 2011). Mus81-Eme1 (Mms4), Yen1 (GEN1), SLX1-SLX4, XPF-ERCC1 and Sgs1/MutL γ /ExoI have cleavage potential and may be used sequentially in a multi-step process. Archaea possess the resolvase Hjc that has a similar function to RuvC and may be used alternately with Hef (archaeal homologue of XPF/Mus81) (Lestini *et al.* 2010).

Choice of DSB repair pathway

Depending on the organism and cell cycle stage, the choice of DSB repair pathway varies. Bacteria primarily use HR (Kowalazykowski et al. 1994) however both NHEJ and HR are utilised in eukaryotes. Repair by HR is restricted to S and G2 phases of the cell cycle where sister chromatids are free to be used as templates for repair following DNA replication (Sonoda et al. 2006; Shrivastav et al. 2008). NHEJ takes place throughout the cell cycle, although it is primarily used during G1 (Shrivastav et al. 2008; Symington & Gautier 2011). During this cell cycle phase DNA end-resection is inhibited, preventing DSB repair by HR. Regulation of repair pathway choice is controlled through phosphorylation of Sae2/CtIP by CDKs (cyclin-dependant kinases) (Blackwood *et al.* 2013). In mammalian cells Mre11 has been shown to interact with CDK2-cyclin A, enabling phosphorylation of CtIP and controlling end resection at DSBs (Buis *et al.* 2012). Most archaea do not posses homologues of Ku70/80 so are thought to favour HR over NHEJ (Aravind & Koonin

2001; Doherty *et al.* 2001). However recent findings indicate that MMEJ is promoted prior to HR in *H. volcanii* during DSB repair (Delmas et al. 2009).

DSB repair pathway choice in eukaryotes is influenced by 53BP1 and BRCA1. 53BP1 interacts with chromatin to promote NHEJ by inhibiting DSB resection and tethering DSBs to facilitate ligation (Chapman et al. 2012). To promote HR, BRCA1 is thought to inhibit 53BP1 activity through direct interaction during S/G2. The Mre11-Rad50 complex also influences DSB repair pathway choice.

1.3. The Mre11-Rad50 complex

The Mre11-Rad50 complex is found in all domains of life (Avavind *et al.* 1999). This repair complex consists of Mre11, Rad50 and Xrs2 in vertebrates or its homologue Nbs1 in yeast (Bressan et al. 1999; Stracker and Petrini 2011). Archaea lack Xrs2 but possess homologues of Mre11 and Rad50 (Blackwood et al. 2013). In many species, the two components of the complex are contained in an operon, which encodes the single-strand DNA nuclease: Mre11 and an ATPase: Rad50 (Paul and Gellert 1998). The latter possesses a long coiled-coil domain with a zinc hook motif at its tip which enables intermolecular interaction between proximate Rad50 molecules and the tethering of DNA ends or chromosomes (Hopfner et al. 2002; De Jager et al. 2001). In *H. volcanii,* this is involved during nucleoid compaction as a response to DNA damage (Delmas *et al.* 2013). Nucleoid reorganisation coordinated by Mre11-Rad50 is thought to aid the localisation of DNA repair proteins to damaged sites, whilst facilitating the search for intact DNA sequences during homologous recombination. Through these processes the complex is thought to accelerate cellular recovery from DNA damage (Delmas *et al.* 2013).

In eukaryotes, Xrs2/Nbs1 mediates interactions between the Mre11-Rad50 and other DNA-repair proteins (Kobayashi et al. 2004). It can recruit the complex to sites of DNA-damage by interacting with histone γH2AX (Kobayashi et al. 2002). Mre11-Rad50 is one of the first proteins to localise at DSBs, where it is believed to tether DNA ends whilst assembling a scaffold (De Jager *et al.* 2004*;* Lisby *et al.* 2004; Moreno-Herrero *et al.* 2005; Williams *et al.* 2008). It plays an important role in

coordinating end-resection where either HR or MMEJ are promoted. However limited end processing will promote NHEJ.

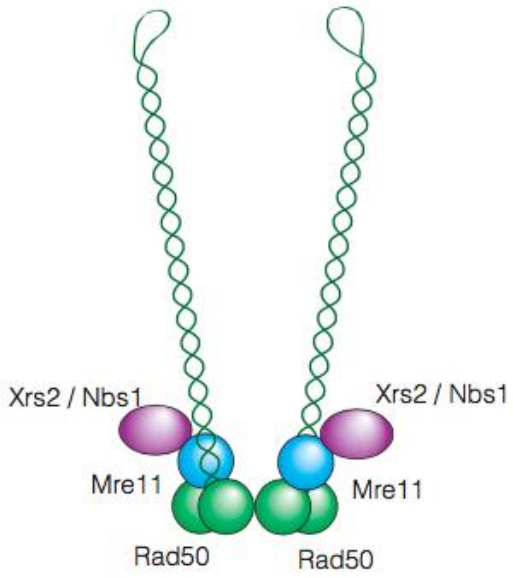

Figure 1.2: **Structure of the eukaryotic Mre11-Rad50 complex**. The complex consists of Mre11 (blue) bound to Rad50 (green) and Xrs2/Nbs1 (purple). Rad50 has a long coiled-coil domain and two ABC domains. It is not known exactly where Xrs2/Nbs1 binds to the complex (Wardell 2013).

HerA & NurA

Xrs2 and Nbs1 are absent from archaea, however the *mre11-rad50* genes are linked to *nurA* and *herA* in most hyperthermophilic archaea, including *Sulfolobus acidocaldarius*, *Sulfolobus islandicus*, Sulfolobus tokodaii (Constantinesco et al. 2002; Constantinesco et al. 2004; Huang et al. 2015; Zhang et al. 2008). *NurA* encodes a nuclease which exhibits both single-stranded endonuclease activity and 5'-3'exonuclease on single and double-stranded DNA. *HerA* encodes a bipolar helicase, which is able to utilize either 3' or 5' single-stranded DNA extension for loading and unwinding the DNA duplex. Together these enzymes form a closed-ring complex (Blackwood et al. 2012). In a manner analogous to bacterial RecBCD, the HerA-NurA complex can degrade both strands of DNA or switch to degrade a single strand to generate an overhang. This is required for recombinase loading and subsequent DNA strand invasion if HR is being used to repair the DSB.

The Mre11-Rad50 complex is also thought to carry out limited end processing preceding extensive resection by HerA and NurA (Hopkins & Paull 2008). However HerA and NurA are both absent from halophilic archaea. *Halobaterium sp.* possess only Mre11 and Rad50 (Kish & DiRuggiero 2008) and the *H. volcanii mre11-rad50* region contains no additional genes in its operon (Delmas et al. 2009). It is therefore currently unknown how this polarity switch from double to single strand degradation is mediated or what carries out extensive end resection in these species of archaea.

1.3.2. DNA damage resistance

The absence of Mre11-Rad50 affects DNA damage resistance differently between species. Null mutations of *sbcCD* in bacteria confer sensitivity to DNA damage in *Deinococcus radiodurans* and *Bacillus subtilis* (Bentchikou *et al.* 2007; Mascarenhas *et al.* 2006). In *S. cerevisiae mre11rad50* mutants show sensitivity to ionizing radiation (Game & Mortimer, 1974). In mice, *rad50* mutants cause embryonic stem cell lethality (Luo *et al.* 1999). Hypomorphic mutations in human Mre11 are present in individuals with ataxia-telangiectasia-like disorder (ATLD) (Stewart *et al.* 1999). However *E. coli sbcCD* mutants and *Halobacterium sp. Mre11rad50* mutants show no increased sensitivity to DNA damage (Lloyd & Buckman, 1985; Connelly & Leach, 2002; Kish & DiRuggiero 2008).

Effect on Homologous Recombination

DSB repair by HR is increased in *H. volcanii* strains deleted for *mre11-rad50* (Delmas et al. 2009). This is in contrast to other systems where HR is decreased by such mutations; *S. cerevisiae* and human cancer cells show defects in HR repair when the complex is mutated (Lewis *et al.* 2004; Krishna *et al.* 2007; Lee *et al.* 2015). These *H. volcanii* mutant strains are also more resistant to UV-irradiation than the wild-type but recover more slowly following treatment (Delmas et al. 2009). This suggests that Mre11-Rad50 is restraining HR at DSBs to allow other repair mechanisms to repair DSBs. *H. volcanii* has been suggested to use MMEJ but other repair mechanisms may be possible. The occurrence of increased DNA damage resistance after mutation of DNA repair genes has been observed in other organisms. NHEJ-defective chicken DT40 and yeast cells have been shown to resist high doses of

γ radiation and phleomycin (Takata *et al.* 1998, Zhang *et al.* 2007). The resistance is believed to be caused by an inability to supress HR (Sonoda *et al.* 2006).

HR is thought to be restrained by Mre11-Rad50 in *H. volcanii,* as the complex does not appear to be actively promoting an alternative repair mechanism (Delmas *et al.* 2009). Assembly of RadA nucleoprotein filaments on ssDNA is essential for stand exchange during HR. The filaments bind to dsDNA and when a homologous region is found, strand invasion and D-loop formation is catalysed (McEntee et al. 1979). *radA* null mutants are sensitive to DNA damage and cannot perform HR (Delmas et al. 2009). However *radA* mutants are no more sensitive than *radAmre11rad50* mutants, indicating that these proteins may be functioning in the same pathway and that HR is ultimately required to repair DNA damage.

Effect of Polyploidy

Organisms with a high genome copy number may experience a greater cost for using HR due to the extended time they need for DSB repair. In polyploid *Halobacterium* sp. NRC-1, slower repair of DSBs has been observed in *mre11* mutant cells (Kish & DiRuggiero, 2008). *D. radiodurans* contains up to 8 copies of its genome and displays a similar phenotype when *sbcCD* is mutated following γ radiation (Bentchikou *et al.* 2007). In *H. volcanii, mre11rad50* mutant cells recover significantly slower following DSB induction through UV irradiation when compared to WT (Delmas *et al.* 2009).

Due to *H. volcanii* being highly polyploid, there is a risk of generating chromosome concatemers, which must be resolved before cell division. When each DSB has 20 partners, repair by HR may be difficult to coordinate. It is therefore advantageous for polyploid organisms to adopt this restraining mechanism to reduce the number of DNA ends and prevent them from engaging with multiple partners. A similar two-step process has been observed in the polyploid bacterium *D. radiodurans,* which uses extended synthesis-dependant strand annealing (ESDSA) to reassemble DNA fragments before HR is used to reconstitute chromosomes (Zahradka et al. 2006). In *H. volcanii,* Mre11-Rad50 could temporarily block the formation of RadA filaments at DSBs to prevent HR so MMEJ can be used. HR may then be used later to repair errors caused by MMEJ.

1.4 Aims

The aim of this study is to identify any protein interactions of the Mre11-Rad50 complex. To achieve this, native *mre11rad50* must be deleted from the *H. volcanii* genome and replaced with a His_6/StrepII-tagged version of *mre11rad50.* This will be expressed using the native promoter and His_6/StrepII-tagged Mre11-Rad50 will be purified on His_6/StrepII affinity columns. Interacting protein partners should co-purify with the complex. Purification will be carried out in the presence of DSBs by incubating cultures with 4NQO (UV mimetic chemical). This approach will reveal whether protein:protein interactions of Mre11-Rad50 change during DSB repair, further elucidating its role in this process.

Chapter 2: Materials and Methods

2.1 Materials

2.1.1. Strains

Details of strain construction are discussed in Chapter 3: *plasmid and Strain Construction*

Haloferax volcanii Strains

Table 2.1 ***H. volcanii*** **strains used in this study**

Strain	Parent	Genotype	Notes
H115	H26	Δ*pyrE2, bgaHa-Kp*	Constructed by TA
H202	H115	Δ*pyrE2, bgaHa-Kp,* Δ*Rad50*	Constructed by TA
H203	H115	Δ*pyrE2, bgaHa-Kp,* Δ*mre11*	Constructed by TA
H204	H115	Δ*pyrE2, bgaHa-Kp,* Δ*mre11Rad50*	Constructed by TA
H2047	H1611	Δ*pyrE2, Nph-pitA,* Δ*mrr, cdc48d-Ct,* Δ*trpA*	Constructed by TA

TA= Thorsten Allers

Escherichia coli Strains

Table 2.2 ***E. coli*** **strains used in this study**

Strain	Genotype	Detail
XL1-Blue MRF	*ndA1, gyrA96* (NalR), *lac* [F'proAB l*acIqZΔM15 Tn10* (TetR)], Δ(*mcrA*)*183*, Δ(*mcrCB-hsdSMR-mrr*)*173*, *recA1*, *relA1*, *supE44*, *thi-1*	Cloning vector for blue/white selection using pBluescript based plasmids. Tetracycline resistant. Restriction, endonuclease and recombination deficient. d*am*+. From Stratagene.

2.1.2 Plasmids

Details of plasmid construction are discussed in Chapter 3: *Plasmid and Strain Construction*

Table 2.3: **Plasmids used in this study.**

Name	Use	Notes
pTA42	*mre11-rad50* genomic clone	Constructed by TA
pTA138	For *mre11-rad50::trpA* deletion construct	Constructed by GN
pTA298	For *mre11-rad50::trpA* deletion construct	Constructed by TA
pTA1560	For construction of genes with His/Strep tag	Constructed by HM
pTA1573	For construction of His/Strep tagged *mre11-rad50*	See Chapter 3 Section 3.1.3
pTA1574	For construction of His/Strep tagged *mre11-rad50*	See Chapter 3 Section 3.1.3
pTA1582	For construction of His/Strep tagged *mre11-rad50*	See Chapter 3 Section 3.1.3
pTA1588	For construction of His/Strep tagged *mre11-rad50*	See Chapter 3 Section 3.1.3
pTA1589	*mre11-rad50::trpA* deletion construct	See Chapter 3 Section 3.1.2
pTA1594	His/Strep tagged *mre11-rad50*	See Chapter 3 Section 3.1.3

TA= Thorsten Allers, GN= Greg Ngo, HM= Hannah Marriott

2.1.3 Oligonucleotides

PCR primers

Details of use will be discussed in Chapter 3

Name	Sequence (5'-3')	Use
Mre11usBsiWF	CGAACCGTaCGCTACGCGCTCTCCCG	Amplify upstream flanking region of *mre11-rad50*
Pmre11R	CCCGTGTCATaTgTCACTCGGTTCG	Amplify upstream flanking region of *mre11-rad50*

mreBspF	GAGTGATtcATGACACGGGTGATACAC	Amplify upstream section *mre11-rad50*
rad50intR	GATTCGAGTTCTCGTTCGGCCTCGG	Amplify upstream section *mre11-rad50*
rad50intF	GAGGACCTGACCGCGAAAATCTCCG	Amplify downstream section *mre11-rad50*
rad50NheR2	GACCGgCtagcGTCGTCCGCGAGCGCGCCTTCG	Amplify downstream section *mre11-rad50*
rad50dsBamF	GGTCGGaTCCGCCGCGATAGCCTACTCGC	Amplify downstream flanking region of *mre11-rad50*
rad50dsNheR	CAACCGCTAgCAGTCGCCGCGCCCTTCGC	Amplify downstream flanking region of *mre11-rad50*
5776R2	GGCGCTCGACAGGCCCATCTCG	Confirm presence of His/StrepII-tagged *mre11-rad50* in H2239
HVR5BF	TCTCGACGCTCGAATCGA	Confirm presence of His/StrepII-tagged *mre11-rad50* in H2239
mreradR	GCGACCTCCACGGTCTCTTG	Confirm presence of His/StrepII-tagged *mre11-rad50* in H2239

Lower case letters indicate mis-matches with the wild-type gene. Novel restriction sites are underlined.

2.1.4 Chemicals and Enzymes

All chemicals were purchased from Sigma and all enzymes from New England Biolabs (NEB), unless stated otherwise. Any chemicals, buffers and solutions used are specified in the appropriate method.

2.1.5. Media

Haloferax volcanii Media

The media was sterilised by autoclaving and stored at room temperature in the dark. Plates were stored in sealed bags in the dark at 4°C to prevent desiccation and were dried for at least 30 minutes before use.

30% salt water (SW): 4 M NaCl, 148 mM $MgCl_2 \cdot 6H_2O$, 122 mM $MgSO_4 \cdot 7H_2O$, 94 mM KCl, 20 mM Tris.HCl pH 7.5.

18% salt water (SW): Made up with 30% SW, 3 mM $CaCl_2$.

$CaCl_2$ added after autoclaving.

Trace elements: 36 mg $MnCl_2.4H_2O$, 44 mg $ZnSO_4.7H_2O$, 230 mg $FeSO_4.7H_2O$, 5 mg $CuSO_4.5H_2O$.

Filter sterilised and stored at 4℃.

Hv-Min salts: 0.4 M NH_4Cl, 0.25 M $CaCl_2$, 8% v/v of trace elements. Store at 4℃.

Hv-Min carbon source: 10% DL-lactic acid Na_2 salt, 9% succinic acid Na_2 salt·$6H_2O$, 1% glycerol, pH to 6.5 with NaOH.

Filter sterilised.

10 × YPC: 5% yeast extract (Difco), 1% peptone (Oxoid), 1% casamino acids, 17.6 mM KOH.

Not autoclaved, used immediately.

10 × Ca: 5% Casamino acids, 23.5 mM KOH. Not autoclaved, used immediately.

Hv-YPC agar: 1.5% Bacto agar (5 g), 18% SW, 1 ×YPC, 3 mM $CaCl_2$.

Microwaved without 10× YPC to dissolve agar. 10× YPC added, then autoclaved. $CaCl_2$ added prior to pouring.

Hv-Ca agar: 1.5% Bacto Agar (5 g), 18% SW, 1 × Ca, 3 mM $CaCl_2$, 36 μg biotin, 288 μg thiamine.

Microwaved without 10× Ca to dissolve agar. 10× Ca added, then autoclaved. $CaCl_2$, thiamine and biotin added prior to pouring.

Hv-Min agar: 5 g Agar (Bacto), 18% SW, 30 mM Tris·HCl pH 7.5, 2.5% Hv-Min carbon source, 1.2% Hv-Min Salts, 325 μM KPO4 buffer (pH 7.5), 444 nM biotin, 2.5 μM thiamine.

Microwaved to dissolve agar. Tris·HCl pH 7.5 added, then autoclaved. Hv-Min carbon source, Hv-Min Salts, KPO4 buffer, biotin and thiamine added prior to pouring.

Hv-YPC broth: 18% SW, 1× YPC, 3 mM $CaCl_2$.

$CaCl_2$ added after autoclaving, when cool.

Hv-Ca+ broth: 18% SW, 22 µM Tris.HCl pH 7.0, 1 ×Ca, 1.9% Hv-Min carbon source,

0.9% Hv-Min Salts, 500 µl 0.5 M KPO_4 buffer (pH 7.5), 444 nM biotin, 2.5 µM thiamine.

30% SW, dH_2O and Tris-HCl pH 7.0 autoclaved. All other components added when cooled.

Haloferax volcanii media supplements

All solutions sterilised by filtration through a 0.2 µm filter.

Table 2.6: **Media supplements used with *H. volcanii***

Supplement	Abbreviation	Final Concentration
Uracil	Ura	50µg/ml
Tryptophan	Trp	50µg/ml
5-Fluoroorotic acid	5-FOA	50µg/ml (+10µg/ml uracil)

Growth of *H. volcanii* auxotrophic mutants on different media: if named the supplement requires addition to the growth media.

Table 2.7: ***H. volcanii* mutant growth in different media.**

Genotype	Hv-YPC	Hv-Ca	Hv-Min
Δ*pyrE2*	+	Ura-	Ura-
Δ*trpA*	+	Trp-	Trp-

Escherichia coli Media

Sterilised by autoclaving and stored at room temperature.

LB (Lysogeny Broth): 1% tryptone (Bacto), 0.5% yeast extract (Difco), 170 mM NaCl, 2 mM NaOH, pH 7.0.

LB agar: 300 ml of LB broth, plus 1.5% agar (4.5 g).*Mu agar:* 1% tryptone (Bacto), 0.5% yeast extract, 340 mM NaCl, 2 mM NaOH

pH 7.0. To 300 ml of broth, 1% agar was added (3 g).

Escherichia coli media supplements

Table 2.9**: Typical cycling conditions for PCR reactions.**

Supplement	Abbreviation	Final concentration
Ampicillin	Amp	50 µg/ml
Tetracyclin	Tet	3.5 µg/ml

2.2 Methods

2.2.1. Haloferax volcanii Microbiology

Growth and Storage

H. volcanii were plated and grown on solid media for 5-10 days at 45°C in a static incubator (LEEC) inside a plastic bag to prevent drying. Small liquid cultures (1-10ml) were grown overnight in the same incubator with 8rpm rotation. Plates and cultures were also temporarily stored at room temperature. For long-term storage, glycerol to 20% (v/v) was added to cultures (as 80% glycerol in 6% SW), mixed and flash frozen on dry ice. Frozen cultures were stored at -80°C.

Transformation using PEG600

PEG600 has been shown to efficiently transform *H. volcanii* (Cline et al. 1989). Prior to transformation DNA requires passage through a dam- E.coli host due to the presence of a restriction endonuclease encoded in *H. volcanii* that targets methylated DNA. However Δ*mrr H. volcanii* strains can be transformed directly with dam+ plasmid DNA.

Buffers and Solutions:

All sterilised by filtration through a 0.2 µM filter.

Buffered Spheroplasting Solution: 1 M NaCl, 27 mM KCl, 50 mM Tris.HCl pH 8.5, 15% sucrose.

Unbuffered Spheroplasting Solution: 1 M NaCl, 27 mM KCl, 15% sucrose, pH 7.5.

Transforming DNA: 5 µl 0.5 M EDTA, pH 8.0, 15 µl unbufferred spheroplasting solution, 10 µl DNA (~1-2 µg).

60% PEG 600: 150 µl PEG 600 and 100 µl unbuffered spheroplasting solution.

Spheroplast Dilution Solution: 23% SW, 15% sucrose, 37.5 mM $CaCl_2$.

Regeneration Solution: 18% SW, 1×YPC, 15% sucrose, 30 mM $CaCl_2$.

Transformation Dilution Solution: 18% SW, 15% sucrose, 30 mM $CaCl_2$.

1-4 colonies were used to inoculate 10ml of Hv-YPC broth and incubated at 45°C for ~16 hours. When the A_{650} = 0.6-0.8, cells were pelleted by centrifugation in a 10 ml round-bottom tube at 3300×*g* for 8 minutes. The supernatant was removed and cells were resuspended in 2 ml of buffered spheroplasting solution and transferred to a fresh 2 ml round-bottom tube. Cells were pelleted again and the supernatant removed. Cells were resuspended gently in 600-800 µl buffered spheroplasting solution. 200 µl of this was used per transformation and transferred to a fresh 2 ml tube. 20 µl of 0.5 M EDTA (pH 8.0) was added, mixed by gentle inversion and incubated at room temperature for 10 minutes to allow removal of the *H. volcanii* S-layer (spheroplasting).

Transforming DNA was added in the same manner as EDTA and incubated at room temperature for 5 minutes. 250 µl of 60% polyethylene glycol 600 (PEG 600) was added and mixed by gentle rocking. The sample was incubated at room temperature for 30 minutes, then diluted with 1.5 ml of spheroplast dilution solution and mixed by inversion. After 2 minutes the cells were pelleted at 3300×*g* for 8 minutes and the cell pellet transferred to a sterile tube containing 1 ml of regeneration solution. To allow recovery of cells, the tube was incubated undisturbed for 90 minutes at 45℃. The pellet was then resuspended by gently tapping the tube and incubated at 45℃ with 8 rpm rotation for 3 hours. Cells were transferred to a fresh 2 ml round-bottom tube and

centrifuged at 3300×*g* for 8 minutes. The cell pellet was resuspended gently in 1ml of transformation dilution solution. Appropriate dilutions were made and 100 µl of each dilution plated on appropriate media. Plates were incubated for at least 5 days at 45°C.

2.2.1. Escherichia coli Microbiology

Growth and Storage

E.coli strains were plated and grown on solid media at 37°C overnight in a static incubator (LEEC). Small liquid cultures (1-10ml) were grown overnight in the this incubator with 8 rpm rotation. Large scale cultures (300ml) were grown overnight in an Innova 4330 floor-standing shaking incubator (new Brunswick Scientific) with 110 rmp shanking*. Plates and cultures were stored short-term at 4°C and for long-term storage, glycerol was added to 20% (v/v) to cultures and mixed then flash frozen on dry ice. Frozen cultures were stored at -80°C.

Electrocompetent E.coli cells

A 5ml culture of XL-1 Blue (dam+, tetracycline resistant) cells was grown overnight at 37°C with 8 rpm rotation with appropriate antibiotic selection. Cells were diluted 1/100 in LB broth supplemented with appropriate antibiotics and grown at 37℃ to A_{650} = 0.5-0.8. Cells were pelleted at 6000×*g* for 12 minutes at 4℃ and the supernatant removed. The pellet was resuspended in an equal volume of ice-cold sterile 1 mM HEPES (pH 7.5). This process was repeated using 0.5 volumes 1 mM HEPES, 0.25 volumes 1 mM HEPES + 10% glycerol, 0.1 volumes 1mM HEPES + 10% glycerol, and finally 0.001 volumes 1mM HEPES + 10% glycerol. Cells were flash frozen on dry ice and stored in 100 µl aliquots at -80℃.

Transformation of Escherichia coli by Electroporation

Buffers and Solutions:

> **SOC broth**: 2% tryptone (Bacto), 0.5% yeast extract (Difco), 10 mM NaCl, 2.5 mM KCl, 10 mM $MgCl_2$, 10 mM $MgSO_4$, 20 mM glucose.

1 µg of DNA in 4 µl sterile dH_2O was added to 50 µl of electrocompetent cells, on

ice. The mixed sample was added to a pre-chilled electroporation cuvette (1 mm electrode gap, GENEFLOW). The cuvette was placed in an *E. coli* gene pulser (BioRad) and subjected to a 1.8 kV pulse. 1 ml of SOC was added immediately and samples were incubated at 37℃ with 8 rpm rotation for 1 hour to allow for recovery. Cells were plated onto Mu +2×Amp plates and incubated at 37℃ overnight.

2.2.3. Manipulation of Nucleic Acids

PCR Amplification

DyNAzyme EXT (Finnzymes) and Phusion were used to amplify DNA using PCR; both are ideal for amplifying templates with high GC content. DyNAzyme EXT was used for diagnostic amplifications and Phusion was used for amplifications requiring high fidelity. All reactions were carried out using a Techne TC-512 thermocycler.

Reaction conditions:

DyNAzyme EXT:	For Phusion:
200 µM of each dNTP	200 µM of each dNTP
0.5 µM of each primer	0.5 µM of each primer
10-50 ng of template DNA	10 ng of template DNA
1× Optimised DyNAzyme Buffer	1x Phusion GC buffer
5% DMSO	3% DMSO
1 U of Dynazyme EXT	1 U of Phusion

Table 2.9: **Typical cycling conditions for PCR reactions**

	Step	**DyNAzyme**	**Phusion**
Cycles: 30	Initial Denaturation	94°C, 120 seconds	98°C, 30 minutes
	Denaturation	94°C, 15 seconds	98°C, 10 seconds
	Annealing	Tm°C, 20 seconds	Tm°C, 15 seconds
	Extension	72°C, 40 seconds/kb	72°C, 20 seconds/kb
	Final Extension	72°C, 10 minutes	72°C, 10 minutes

Annealing temperatures for primers (Tm℃) were calculated using the following equation (Howley *et al.* 1979) (Fig. 2.1).

$$81.5+\left(16.6\times\log_{10}\left[Na^{+}\right]\right)+(0.41\times\%GC)\text{-}(100\text{-}\%homology)\text{-}\left(\frac{600}{length(bp)}\right)$$

Figure 2.1: **Calculating annealing temperature of primers.** Homology: percentage homology shared between primer and template. Length: length of the primer in base pairs. %GC: percentage guanine and cytosine in the primer.

Touchdown PCR (Amplification of templates with <100% homology to primer)

Two separate annealing temperatures were calculated when primers were not 100% homologous to the template DNA (e.g. introducing restriction sites or mutations). The first was based on the original percentage of homology (Tm_S), and the second on 100% homology (Tm_e). The reaction annealing temperature started at Tm_S and increased to Tm_e across 10 cycles. The remaining 20 cycles used Tm_e as the annealing temperature.

Colony PCR (Amplification of templates from cells)

In order to screen a colony of cells for a desired plasmid, colony PCRs were used. *H. volcanii* colonies growing on solid media were cultured overnight in YPC broth (10ml). 1ml of this culture was pelleted and suspended in 400µl dH_2O. This was boiled at 100℃ to lyse cells then cooled on ice. 1µl of this was then used in a PCR reaction with DyNAzyme EXT polymerase.

Restriction Digests

Digests were carried out as by the manufacturer's instructions (NEB). For double digests, NEB buffers were selected such that each enzyme had at least 75% activity. Plasmid DNA was digested for at least one hour, and genomic DNA for 16 hours. All digests were supplemented with 200 ng/µl BSA (NEB).

Blunt-end Filling with Klenow

Overhangs generated by restriction digests were filled-in to produce blunt ends (before ligation of trpA to pTA138) using Klenow 3'to 5' exo- (NEB). Samples were

incubated with 1 unit of Klenow exo- per µg of DNA, 1 x NEB Buffer 2 and 1 mM dNTPs for 15 minutes at 25℃. The reaction was stopped by the addition to 10 mM (final concentration) of EDTA and heat inactivation at 75℃ for 20 minutes.

Dephosphorylation of Vector DNA

To prevent self-ligation of vector DNA, Antarctic phosphatase was used to remove 5′ phosphate groups. Samples were incubated with 5 units of Antarctic phosphatase/µg of DNA and 1× Antarctic phosphatase buffer for 30 minutes at 37℃. Antarctic phosphatase was heat inactivated at 65℃ for 5 minutes.

Ligation of DNA

Ligations were performed using T4 DNA ligase. For each µg of DNA 5 units of ligase were used in a reaction with 1× T4 ligase buffer. For vector: insert ligations, reactions contained a molar ratio of ~3:1 insert to vector DNA. Ligations were carried out at 15℃ overnight or 4℃ for 36 hours, followed by ethanol precipitation and resuspension in 4µl dH_2O. For blunt ended ligations 1Mm Hexamine cobalt was added to improve the chances of ligation.

Ethanol Precipitation of DNA

Ethanol precipitation was used to concentrate DNA samples. 1/10 volume of 3 M sodium acetate (pH 5.3) and 2 volumes of 100% ethanol were added to DNA samples and incubated at -20℃ for 1 hour. Samples were centrifuged at 4℃, 20,000 ×*g* for 30 minutes and the supernatant removed. Pellets were washed in 400 µl of 70% ethanol followed by centrifugation at 4℃, 20,000 ×*g* for 10 minutes. The supernatant was removed and pellets air-dried before resuspension in sterile dH_2O (4µl for transformations).

Nucleic Acid Purification

PCR products, ligations, restriction digests and dephosphorylated DNA products were purified using Macherey-Nagel DNA purification kits. These kits purify DNA by salt and pH dependent adsorption of DNA to a silica-gel membrane to separate the desired nucleic acid from small oligonucleotides and proteins. DNA was eluted in 30 µl of the provided elution buffer.

DNA Sequencing

The Biopolymer Synthesis and Analysis Unit, University of Nottingham, carried out all sequencing reactions and analysis. Sequencing was carried out using the dideoxy chain termination method (Sanger *et al.* 1977).

Oligonucleotide Synthesis

Oligonucleotides were synthesised either by the Biopolymer Synthesis and Analysis Unit, University of Nottingham, or by Eurofins MWG, Germany.

Nucleic Acid Quantification

The concentration of plasmid preparations was measured using the 260 nm, 280 nm absorbance ratio from spectrophotometer measurements (Beckman Coulter DU 530).

2.2.4. Gel Electrophoresis

Agarose Gel Electrophoresis

Buffers and Solutions:

TBE (Tris/Borate/EDTA): 89 mM Tris.HCl, 89 mM boric acid, 2 mM EDTA.

Loading Dye (5×): 50 mM Tris·HCl, 100 mM EDTA, 15% Ficoll (w/v), 0.25% Bromophenol Blue (w/v), 0.25% Xylene Cyanol FF (w/v).

TBE buffer was used to cast and run agarose gels as is standard practice.

Agarose gels were cast using AGTC Bioproducts Ltd hi-res standard agarose powder and TBE buffer. Ethidium bromide was added to a final concentration of 0.5 μg/ml to allow for visualisation of bands. Gels for size-based DNA extraction were post-stained with ethidium bromide after removal of sample lanes. DNA samples were mixed with a 1/5 by final volume of 5× gel loading dye and loaded alongside either a 1Kb ladder (NEB) or a 100bp ladder (NEB). TBE gels (10cm) were run at 100 V for 1 hour.

Agarose Gel Extraction and Purification of DNA

Sample lanes were protected using foil while the appropriate band was excised to

allow for purification of DNA from agarose gels without UV exposure. DNA was visualised by UV light using a UV transilluminator (UVP inc.). DNA was purified using the Macherey-Nagel DNA purification kit.

SDS-Polyacrylamide Gel Electrophoresis

Buffers and solutions

12.5% SDS-PAGE gel (resolving): 30% acrylamide/bisacrylamide Protogel (National Diagnostics), 1.5 M Tris (pH 8.8), 0.4% SDS 0.05% AMPS (ammonium persulfate), 0.05% TEMED (tetramethyleethylenediamine), , 2.46ml H_2O.

3.0% SDS-PAGE gel (stacking): 30% acrylamide/bisacrylamide Protogel, 0.5 M Tris (pH 6.8), 0.5% SDS, 0.125% AMPS, 0.125% TEMED, 0.77ml H_2O.

SDS-PAGE running buffer: 0.25 M Tris, 1.92 M glycine, 1% SDS.

Laemmli buffer (4×): 50mM Tris pH 6.8, 100 mM DTT, 2% SDS, 0.1% bromophenol blue, 10% glycerol.

Protein samples were analysed using SDS-PAGE (sodium dodecyl sulphate polyacrylamide gel electrophoresis). Gels were made in Novex cassettes (Invitrogen). A 12.5% resolving gel was poured with a layer of isopropanol on top to flatten the surface. Once set, the isopropanol was washed off and a 3% stacking gel poured with a comb inserted. Protein samples were mixed with a 1/4 by final volume of 4× Laemmli buffer, denatured by boiling at 94℃ for 5 minutes and run alongside a PageRuler size ladder (Fermentas). Gels were run for ~1 hour 30 minutes in 1× SDS-PAGE running buffer (200 V, 36 mA per gel) and stained with PageBlue Protein Staining Solution (Thermo Scientific) for visualization of proteins.

2.2.5. DNA Extraction From Cells

Plasmid Extraction from Escherichia coli

To obtain circular plasmid DNA from *E. coli*, Macherey-Nagel Nucleospin (Mini) /

Nucleobond AX (Midi) kits were used. Minipreps were carried out when large yields of plasmid DNA were not required (e.g. verification of plasmids by restriction digest). Midiprep kits were used when large, ultra-pure DNA yields were required, (e.g. for frozen plasmid stocks).

E. coli strains were grown overnight at 37℃ in LB broth (+Amp), 1 ml of cell culture was used for minipreps, and 300 ml for midipreps. Protocols used were as described in the manufacturer's guidelines. The kits use standard alkaline lysis and salt and pH dependent adsorption of DNA to a silica-gel membrane to separate from nucleotides and proteins, followed by elution. Plasmid DNA from minipreps was eluted in 30 µl elution buffer, and from midipreps plasmid DNA was ethanol precipitated and resuspended in 200 µl of TE. Plasmid DNA samples were stored at -20℃.

2.2.6. Genetic Manipulation of Haloferax volcanii

Gene deletion / Replacement

H. volcanii Δ*pyrE2* strains were transformed with the deletion construct and plated onto Hv-Ca to select for integration of the *pyrE2*-marked plasmid (*pyrE2*+, pop-in). After 5 days growth, pop-in colonies were restreaked onto the same media. In order to allow for popout, a 5 ml Hv-YPC culture was inoculated from a single colony and the culture allowed to grow non-selectively until $A_{650} \approx 1.0$ (stationary phase). The culture was then diluted 1/500 into a fresh Hv-YPC culture and the growth and dilution repeated. When the third culture reached an $A_{650} \approx 1.0$ the culture was diluted and plated into Hv-Ca +5-FOA (+ appropriate additives depending on the strain) to select for pop-outs (*pyrE2*-). Colonies were restreaked onto selective media and tested for the desired genotype. Strains transformed with a trpA-marked deletion construct that was subsequently replaced could be screened by patching out on YPC to test for the presence of the marker. This will be discussed in more detail in Chapter 3: *Construction of Plasmids & Strains.*

2.2.7. Genotype Screening

To screen for the presence or absence of a gene there are a number of techniques used. Firstly, if the strain has a selectable phenotype (e.g. Δ*trpA* strain) then candidate colonies can be plated onto selective media. Due to the polyploid nature of *H.*

volcanii, strains can be merodiploid with chromosomes having a mixture of wild-type and mutant alleles. Therefore, in order to screen for strains in which all chromosomal alleles are the same, colony hybridization or Southern blotting is used. For gene deletions, the absence of a gene is screened for. For both of these methods, DNA was denatured and transferred to a positively charged membrane by either colony lift or vacuum transfer (respectively).

Colony Lift

Buffers and solutions:

20*×*SSPE: 3 M NaCl, 230 mM NaH_2PO_4, 32 mM EDTA, pH 7.4.

Denaturing Solution: 1.5 M NaCl, 0.5 M NaOH.

Neutralising Buffer: 1.5 M NaCl, 0.5 M Tris·HCl, 1 mM EDTA.

In order to allow for screening of large numbers of colonies of interest by colony hybridization, colony lifts were performed. Candidate colonies and controls were patched on to Hv-YPC (+Thy if required) plates using sterile sticks and incubated at 45℃ until grown (~3 days). Bio-Rad Zeta-Probe GT positively charged membrane was left on the plate surface for 1 minute. Membrane was transferred colony side up to Whatman paper soaked in 10% SDS for 3 minutes to lyse cells. The membrane was then transferred to Whatman paper soaked in denaturing solution for 5 minutes to denature proteins and DNA then transferred to Whatman paper soaked in neutralising solution for 3 minutes. Neutralisation was repeated and the filter was washed briefly (30 seconds) in 2×SSPE before being air-dried on Whatman paper. DNA was crosslinked to membrane with UV (120 mJ/cm^2).

Hybridisation

Buffers and solutions:

100*× *Denhardt's Solution: 2% Ficoll 400, 2% PVP (polyvinyl pyrrolidone) 360, 2% BSA (bovine serum albumin, Fraction V).

20*×*SSPE: 3 M NaCl, 230 mM NaH_2PO_4, 32 mM EDTA, pH 7.4.

Prehybridisation Solution: 6× SSPE, 1% SDS, 5x Denhardts, 200µg/ml Fish DNA (Fish DNA boiled for 5 minutes prior to addition).

Hybridisation Solution: 6× SSPE, 1% SDS, 5% dextran sulphate.

Low Stringency Wash Solution: 2× SSPE, 0.5% SDS.***High Stringency Wash Solution***: 0.2× SSPE, 0.5% SDS.

Membranes were transferred to a Hybaid tube with 40 ml of prehybridisation solution, and incubated at 65℃ for 3 hours. Radiolabelled DNA probes were made with 50 ng of DNA and 0.74 Mbq of α[^{32}P] dCTP (GE Healthcare, Amersham Redivue). DNA was denatured at 100℃ for 5 minutes then incubated with the radioisotope and HiPrime random priming mix (Roche) for 15 minutes at 37℃. The radiolabelled probe was then purified on a BioRad P-30 column and mixed with 10 mg/ml of Fish sperm DNA (Roche) followed by denaturing at 100℃ for 5 minutes and quenching on ice. For Southern blots, 1 µl of 1µg/ml 1 Kb ladder was also included in the radiolabelling reaction. The prehybridiation solution in the Hybaid tube was replaced with 40 ml of hybridisation solution, and the probe DNA added. Membranes were incubated overnight at 65℃. The membranes were washed twice with 50 ml of low stringency wash solution (10 minutes then 30 minutes) followed by another two washes with high stringency wash solution (both 30 minutes). Membranes were allowed to dry before been wrapped in Saran wrap and exposed to a phosphorimager screen (Fujifilm BAS Cassette 2325) for >24 hours. The screen was scanned using a Molecular Dynamics STORM 840 scanner.

2.2.8. Phenotyping of *H. volcanii*

DNA-Damage Assays

To determine the optimal concentration of mutagen to give 90% survival of *H. volcanii,* assays were performed using a number of DNA damaging agents.

UV-Irradiation

5 ml of HV-YPC broth was inoculated and grown at 45℃ in two successive dilutions, to an OD of $A_{650} \approx 0.35$-0.4 (mid-exponential phase). 1 ml of culture used in appropriate serial dilutions in 18% salt water. Duplicate 20 µl spots were spotted out on Hv-YPC agar (+Thy if required) and allowed to dry at room temperature. Plates were exposed to UV light (254mM, 1 J/m^2/sec) and shielded from visible light to prevent photo-reactivation. Colonies were counted after 4-7 days incubation at 45℃. Survival fractions were calculated relative to an unirradiated control.

Chemical Mutagens

Acute exposure

5ml of Hv-YPC broth was inoculated and grown at 45℃ in two successive dilutions, to an OD of $A_{650} \approx 0.35$-0.4 (mid-exponential phase). Different strains were split into 1 ml aliquots and 4NQO added. Samples were incubated for 1 hour at 45℃ with 8 rpm rotation, then pelleted and washed to remove the mutagen. Serial dilutions were performed and 20 µl of each dilution was spotted on Hv-YPC agar and dried at room temperature. Colonies were counted after 5-10 days incubation at 45℃. Survival fractions were calculated relative to an untreated control.

Chronic exposure

Mitomycin C sensitivity was analysed as a chronic exposure, with MMC in the agar plates. Cultures were grown as with acute exposure, but instead of treating with toxins in liquid, cells were spotted directly onto Hv-YPC agar (+Thy if required) containing 0-0.03 µg/ml of MMC. Plates were made fresh and used within 5 days.

2.2.9. Native Protein Expression and Purification

Buffers and solutions:

Binding Buffer A: 20 mM HEPES pH 7.5, 2M NaCl, 1mM PMSF (For His purification) or 1x Sigma*FAST (*For protease inhibition), imidizole to desired concentration.

Binding Buffer B: 20 mM HEPES pH 7.5, 2M NaCl, 1mM PMSF (For His purification) or 1x Sigma*FAST (*For protease inhibition), imidizole to desired concentration. 0.016g D-desthiobiotin added for elution buffer.

Native Protein Expression

A starter culture was grown for 8 hours in 5 ml Hv-YPC broth then diluted 1/100 into 50 ml of Hv-YPC broth. When $A_{650} \approx 0.1$ was reached, the culture was diluted 1/200 in Hv-YPC broth and incubated at 45°C with shaking (150 rpm) for 24 hours. For Large-scale cultures (for protein purification) 2 L of Hv-YPC was used. The culture was then pelleted at 6000 rpm for 10 minutes at 4℃. Cells were resuspended in ice-

cold Binding Buffer A (20 mM imidazole) and lysed by sonication (2-6×30 sec at ≤ 8μ) on ice. The cell lysate was then transferred to a 15 ml round bottomed tube and centrifuged at 20,000 ×*g* for 30 minutes at 4℃. Sample was filtered sequentially through a 0.2 μM, a 0.45 μM and a 0.8 μM filter.

Purification Using a Ni^{2+} gravity column

Charging of Ni^{2+} beads

IMAC Sepharose 6 Fast Flow beads (GE Healthcare) were charged with Ni^{2+} to allow purification of His_6-tagged proteins. 100 μl of beads were used for small-scale cultures, and 0.5 ml for large scale. Beads were washed twice with >2 column volumes (cv) of dH_2O, then equilibrated for 30 minutes with >0.2 cv of 0.2 M $NiSO_4$. Two washes with >2 cv of dH_2O were performed followed by a further three washes with Binding Buffer A (20mM imidazole) and one wash with Binding Buffer A (500 mM imidazole). Washes with Buffer A were performed to minimize metal ion leakage. Beads were resuspended in 1 cv Binding Buffer A (20mM imidazole).

Ni^{2+} gravity column

Cell lysates were incubated for at least 1 hour at 4℃ with Ni^{2+}-charged IMAC Sepharose 6 FastFlow beads. The beads were applied to a Poly-Prep column (Bio-Rad) and the flow-through collected and reloaded onto the column, followed by three washes with 5 ml of ice-cold Binding Buffer A (20 mM imidazole). Bound protein was eluted with 3 column volumes of binding buffer containing 50, 200 and 500 mM imidazole.

Purification using Strep-Tactin gravity column

1ml IBA Strep-Tactin Sepharose were applied to a Poly-Prep column (Bio-Rad) and was equilibrated with 4ml Buffer B. Cell lysate was applied to the column and the flow-through collected and reloaded onto the column followed by five washes with 1ml Buffer B. Bound protein was eluted with 3 column volumes of elution buffer (B + 5mM desthiobiotin) at 0.8ml, 1.4ml and 0.8ml.

Protein Concentration

Protein samples were concentrated using Vivaspin ultrafiltration spin columns (GE healthcare), which use membrane ultrafiltration to concentrate samples. A molecular weight cut off (MWCO) appropriate to the protein was selected. Protein samples were added to a Vivaspin column that had been washed with 5ml dH_2O and pre-equilibrated with 5ml Binding Buffer B, then spun at 4000 rpm until the desired final volume was reached.

Protein Precipitation

To further concentrate protein samples, a clean up precipitation procedure was used for small scale samples (1-100µg). 300µl 10% TCA was added to each sample and incubated on ice for 5 mins. 300µl of 0.1% DOC was added and incubated for 5 mins. Samples were centrifuged for 5 mins at 12,000 xg and 'pulse' spun to remove supernatant. 40µl 0.05% DOC was added to the pellet, centrifuged for 5 mins and 'pulse' spun. 50µl dH_2O was added and pellet dispersed by vortexing. 1 ml Acetone (pre-chilled -20℃) was added and the pellet vortexed. Samples were incubated for 1 hour at -20℃ and vortexed every 10 mins, then centrifuged at 12,000 xg for 5 mins. Supernatant was discarded and samples resuspended in 20 µl Laemmli buffer (4x).

Chapter 3: Construction of Plasmids and Strains

3.1. Overview

To identify protein interactions of the Mre11-Rad50 complex in *H. volcanii*, firstly a gene knockout system was used to replace the native *mre11rad50* with a *trpA*-marked deletion construct (pTA1589). Secondly a plasmid containing *mre11rad50* with its flanking regions of homology and a His_6/StrepII tag was generated (pTA1594). The strain containing pTA1589 (H2110) was transformed with pTA1594. This generated a strain (H2239) that could be used to express His_6/StrepII-tagged *mre11rad50* in *H. volcanii* using its native promoter. His_6/StrepII-tagged Mre11-Rad50 was purified from cell lysate samples on His_6 and StrepII gravity columns.

3.1.1 Genomic Clones

Genetic manipulation can be performed more easily using plasmids from a library of genomic clones. Only the gene of interest and its upstream and downstream flanking regions are present in each plasmid. By using genomic clones the possibility of PCR errors is significantly reduced when compared to using the whole genome as a template. The genomic clone of the His/Strep-tagged Mre11Rad50 gene was constructed in *E.coli* XL1-Blue due to its short culturing time.

3.1.2. Gene Deletion / Replacement Plasmids

Gene deletion / replacements were performed in *H. volcanii* using the pop-in / pop-out method (Bitan-Banin *et al.* 2003). The plasmids used for gene deletions /replacements (pTA1560 & pTA138) contained *pyrE2* (encodes for orotate phosphoribosyl transferase, an enzyme involved in uracil biosynthesis). Since Δ*pyrE2* strains cannot grow on Hv-Ca media lacking uracil, it is used to select for *H. volcanii*. Deletions can also be marked with *trpA* to allow for additional selection.

Construction of *trpA*-marked deletion construct for native *H. volcanii* Mre11Rad50

In order to delete native *mre11rad50* from *H. volcanii,* a *trpA*-marked deletion construct was generated. The *trpA* marker is used to directly select for strains that have been successfully transformed with the deletion construct (Allers *et al.* 2004) (Fig. 3.9). These strains will be auxotrophic for tryptophan so can be directly selected for on media Hv-Ca media. The plasmid pTA1589 contained the upstream and downstream flanking regions of *mre11rad50,* with the *mre11rad50* operon replaced with *trpA*. *Mre11rad50* will be deleted if the flanking region of homology between the deletion construct and the *H. volcanii* chromosome recombine upstream of the gene (Fig 3.9). The genomic clone pTA138 is a derivative of pTA42 (containing *mre11rad50*) and is deleted for *mre11* but contains *rad50*. To create a *trpA*-marked deletion construct for *mre11-rad50*, the rad50 operon was replaced with a *trpA* marker. pTA1589 was used to replace the wild-type *mre11Rad50* from H2047.

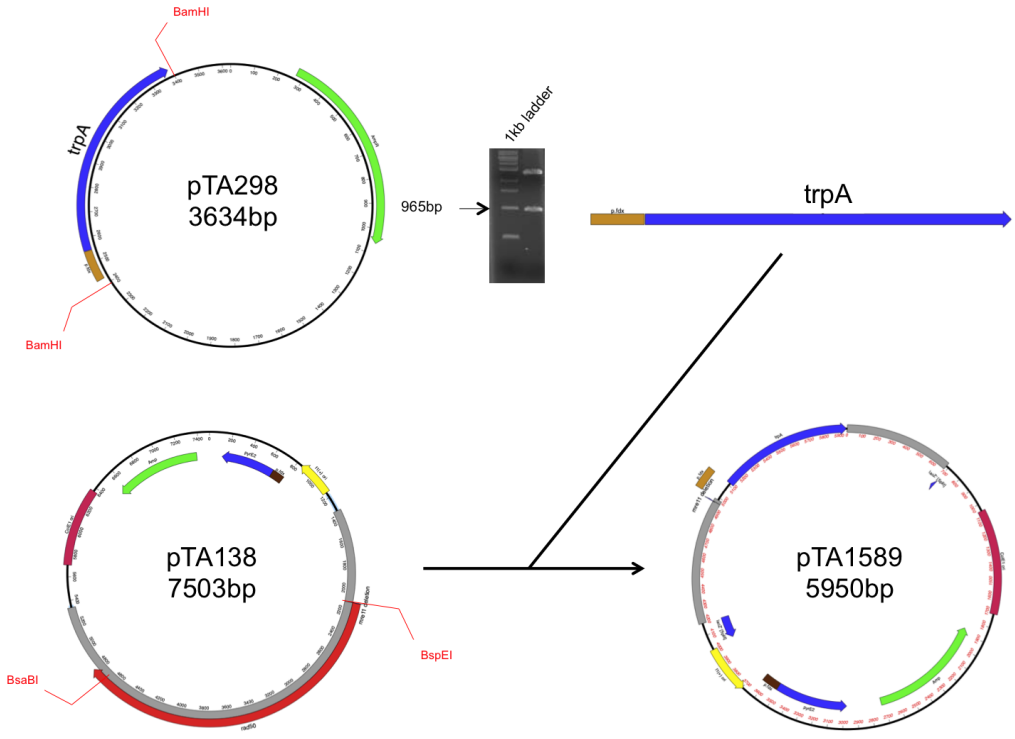

Figure 3.1. **Construction of pTA1589, *mre11rad50* deletion construct. (A)** pTA298 cut with BamHI to obtain *trpA* marker which was blunt-ended with Klenow. **(B)** pTA138 cut with BspEI & BsaBI to remove *rad50.* Sticky ends of the backbone were blunt-ended with Klenow and dephosphorylated with Antarctic phosphatase. Blunt-ended trpA marker was inserted into pTA138 backbone with hexamine cobalt to aid the ligation.

The Rad50 coding sequence had restriction sites available at the 5' and 3' (BsaBI & BspEI) end but did not produce compatible ends after restriction digest. Therefore Klenow polymerase was used to fill in the ends, making them blunt. The genomic clone pTA298 was digested with BamHI, as there are two sites for this enzyme to cut either side of a *trpA* maker. These products were ligated together to create a deletion construct selectable for tryptophan.

3.1.3. Episomal Plasmids for Native Expression of Proteins

The plasmid used to express His_6/StrepII-tagged *mre11rad50* (pTA1594) was derived from pTA1560, a plasmid designed for the expression of double tagged genes under the native promoter on the *H. volcanii* chromosome. pTA1560 was derived from pTA1392 which contains a His_6/StrepII cassette flanked by restriction sites that allow for in-frame insertion of a gene of interest. The gene is controlled using a *p.tnaA*, a tryptophan-inducible promoter (Large *et al.* 2007) to allow for conditional overexpression of *H. volcanii* proteins. pTA1560 lacks *p.tnaA* but contains a *pyrE2* marker, allowing for uracil selection of Hv-Ca media (Fig. 3.8).

Construction of His_6/StrepII -tagged *Mre11Rad50* (pTA1594)

The genomic clone pTA42 contains *mre11rad50* along with its immediate flanking regions. In order to create a His_6/StrepII-tagged version of *mre11rad50* (pTA1594), the operon was ligated to pTA1560 which contains a His_6/StrepII cassette. pTA1594 will be used to replace pTA1589 from the *H. volcanii* chromosome. The plasmid construct will contain the upstream and downstream chromosomal flanking regions of *mre11rad50.* The *trpA*-marked deletion construct will be deleted from *H. volcanii* if the flanking region of homology between the p1594 and pTA1589 recombine upstream of *trpA* (Fig. 3.10). His_6/StrepII-tagged *mre11rad50* will be expressed from the wild-type loci and be under the control of a native promoter.

PCR

The genomic clone pTA42 was used as a template to amplify *mre11rad50* by PCR using mreBspF and rad50NheR. Initially the whole operon (4kb) could not be amplified due to failure of the 5' primer (rad50NheR) to anneal to the correct position

on the template. Two other sites within the operon shared a significant number of bases with the desired annealing site. These factors caused rad50NheR to repeatedly bind to these two separate positions, amplifying 900bp and 1.6kb fragments (Fig. 3.2). Therefore, a second reverse primer (rad50NheR2) was designed with added bases to increase the specificity for the desired annealing site. This primer encountered the same problem so a new cloning strategy was adopted.

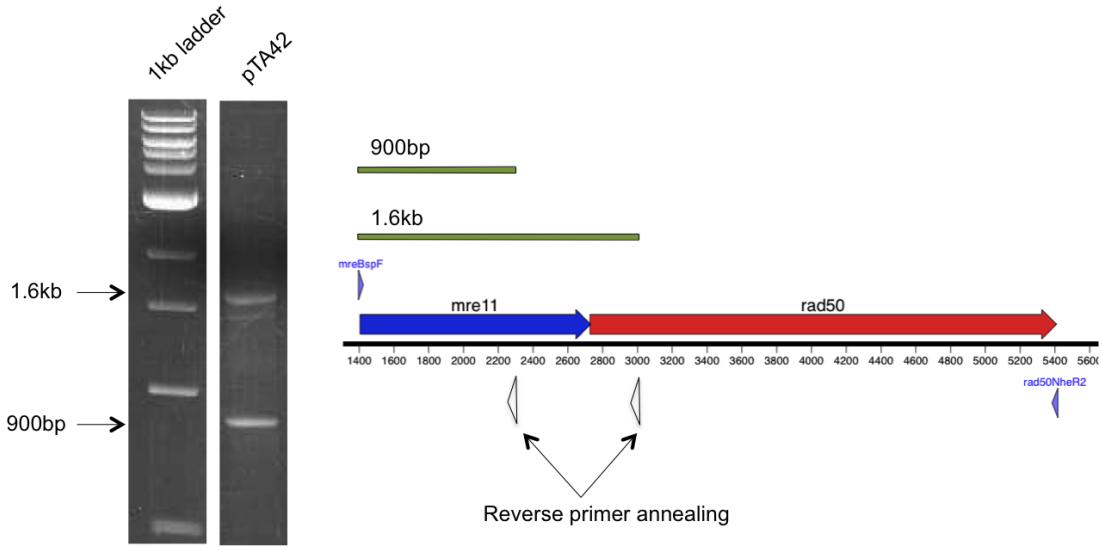

Figure 3.2**. PCR errors made due to failure of reverse primers to anneal to correct site on pTA42.** PCR failed to amplify whole *mre11rad50* operon. When Rad50NheR & Rad50NheR2 were paired with mreBspF, 1.6kb and 900bp products were amplified.

The upstream and downstream halves of *mre11rad50* were amplified separately using internal primers (rad50intF, rad50intR). The two halves of *mre11rad50* were then cloned into two separate vectors (pTA1573, pTA1574) (Fig. 3.3). Separate PCRs were performed to amplify the upstream and downstream flanking regions of *mre11rad50* (Fig 3.5; Fig. 3.6).

Oligonucleotides & Restriction Digest

The forward primer used to amplify *mre11rad50* (mreBspF) contains a BspHI restriction site and the reverse primer (rad50NheR) an NheI site. Because rad50NheR failed to anneal to the desired site, the internal primer rad50intR was paired with mreBspF to amplify the upstream half of the operon and rad50intF was paired with

rad50NheR2 to amplify the downstream half. This set of internal primers was specifically designed to anneal either side of a StuI site (Fig. 3.3).

The upstream fragment was digested and ligated into pTA1560 to create pTA1573 and the downstream fragment into a separate vector (using pTA1560) to create pTA1574 (Fig. 3.3). These plasmids were digested with StuI and HindIII so the upstream fragment from pTA1573 could be inserted into pTA1574. The new plasmid construct (pTA1582) now contained the whole *mre11rad50* operon (Fig. 3.4).

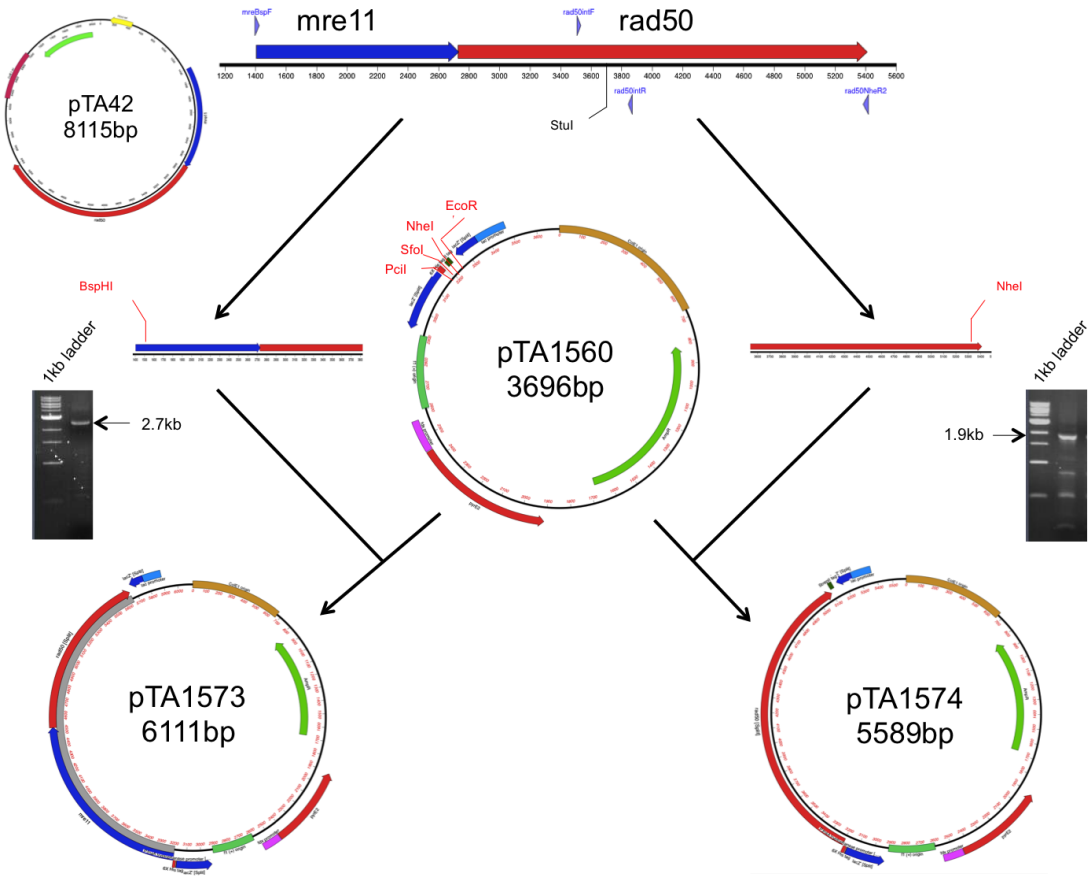

Figure 3.3. **Construction of pTA1573 & pTA1574.** PCR was used to amplify the *mre11rad50* operon from pTA42 using mreBspF & rad50intR (Upstream) and rad50intF & rad50NheR2 (Downstream). PCR products were digested with BspHI (Upstream) and NheI (Downstream) and inserted separately into pTA1560. The upstream product was inserted into EcoRV & PciI sites to generate pTA1573 and the downstream product was inserted into NheI & SfoI sites to generate pTA1574.

The forward primer used to amplify the upstream flanking region (mre11usBsiWF) was designed with a BsiWI site and the reverse primer (pmre11R) an NdeI site. The forward primer used to amplify the downstream flanking region (rad50dsBamF) was designed with a BamHI site and the reverse primer (rad50dsNheR) an NheI site. These oligonucleotides with novel restriction sites were utilised to aid the insertion of the upstream and downstream flanking regions of *mre11rad50* into pTA1582 to create pTA1588 and pTA1594 respectively (Fig. 3.5; Fig. 3.6) Δ*mrr H. volcanii* strains possess the ability to be transformed directly with dam+ plasmid DNA; therefore pTA1594 was used for transformation instead of passaging the plasmid through dam- *E.coli.*

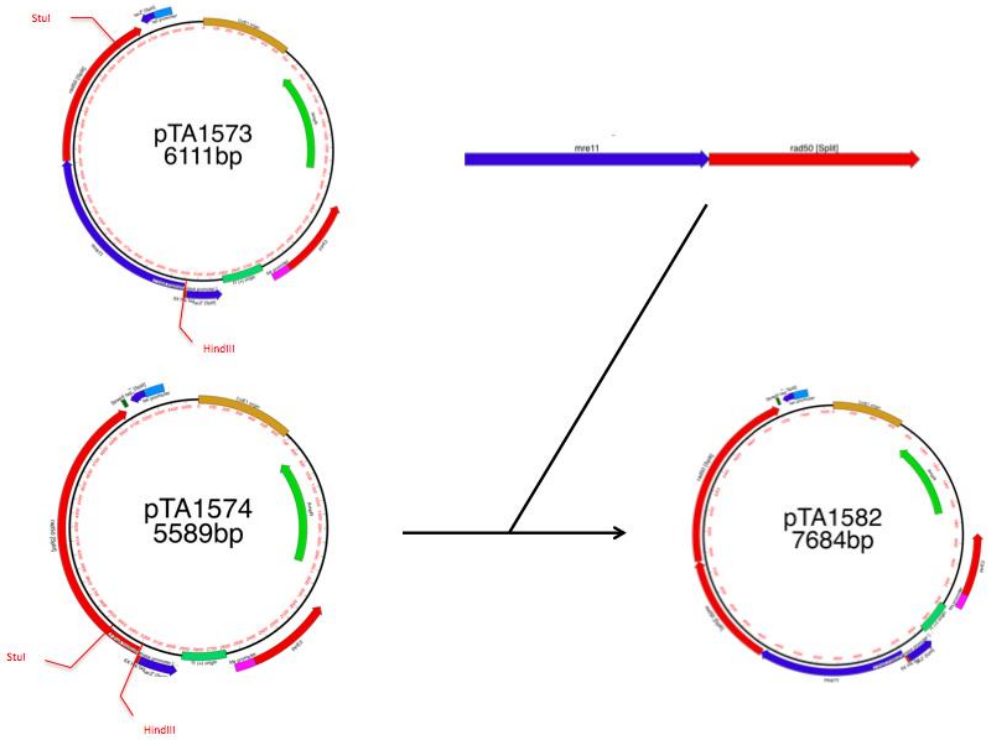

Figure 3.4**. Construction of pTA1582.** pTA1574 & pTA1573 were cut with StuI & HindIII. This separated the upstream section of *mre11rad50* from pTA1573 which was inserted into pTA1574 to generate pTA1582. This plasmid contained the whole *mre11rad50* operon without its upstream and downstream flanking regions.

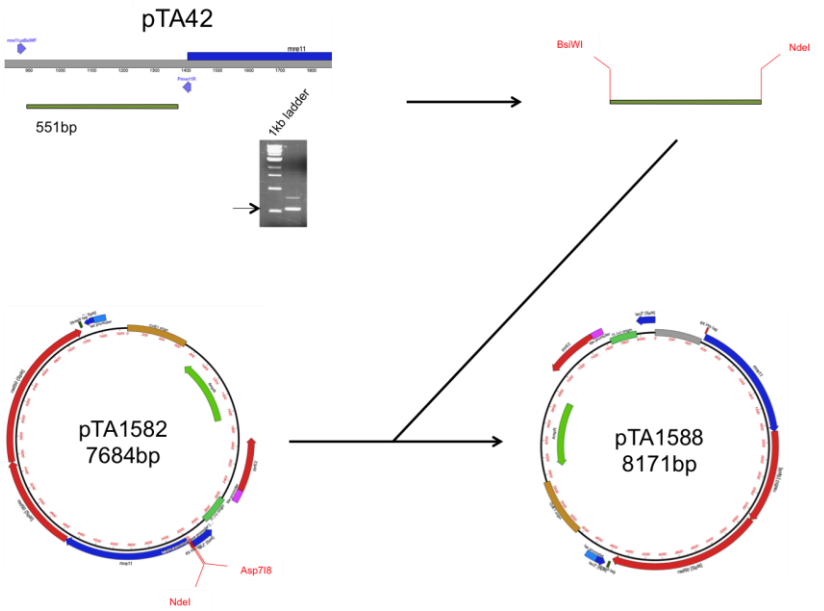

Figure 3.5: **Construction of pTA1588.** PCR was used to amplify the upstream flanking region from pTA42. This PCR product was digested with BsiWI & NdeI and inserted into Asp718 & NdeI sites in pTA1582 to generate pTA1588.

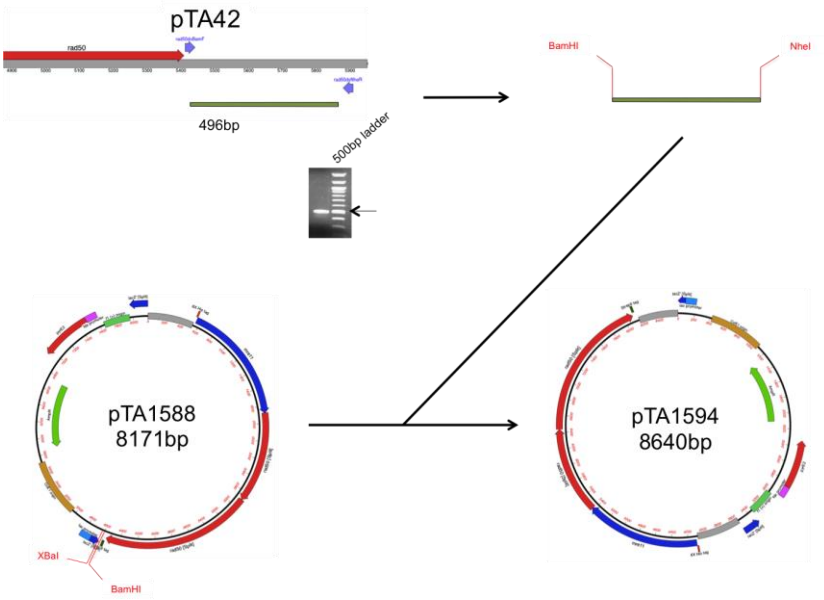

Figure 3.6 **Construction of pTA1594**: PCR was used to amplify the downstream flanking region from pTA42. This PCR product was was digested with NheI & BamHI and inserted into XbaI & BamHI sites in pTA1588 to generate pTA1594.

3.1.4. Confirmation of Plasmids

All plasmids were confirmed by performing restriction digests using a range of restriction endonucleases (Fig. 3.7). For further confirmation, plasmids were sequenced through Source Bioscience.

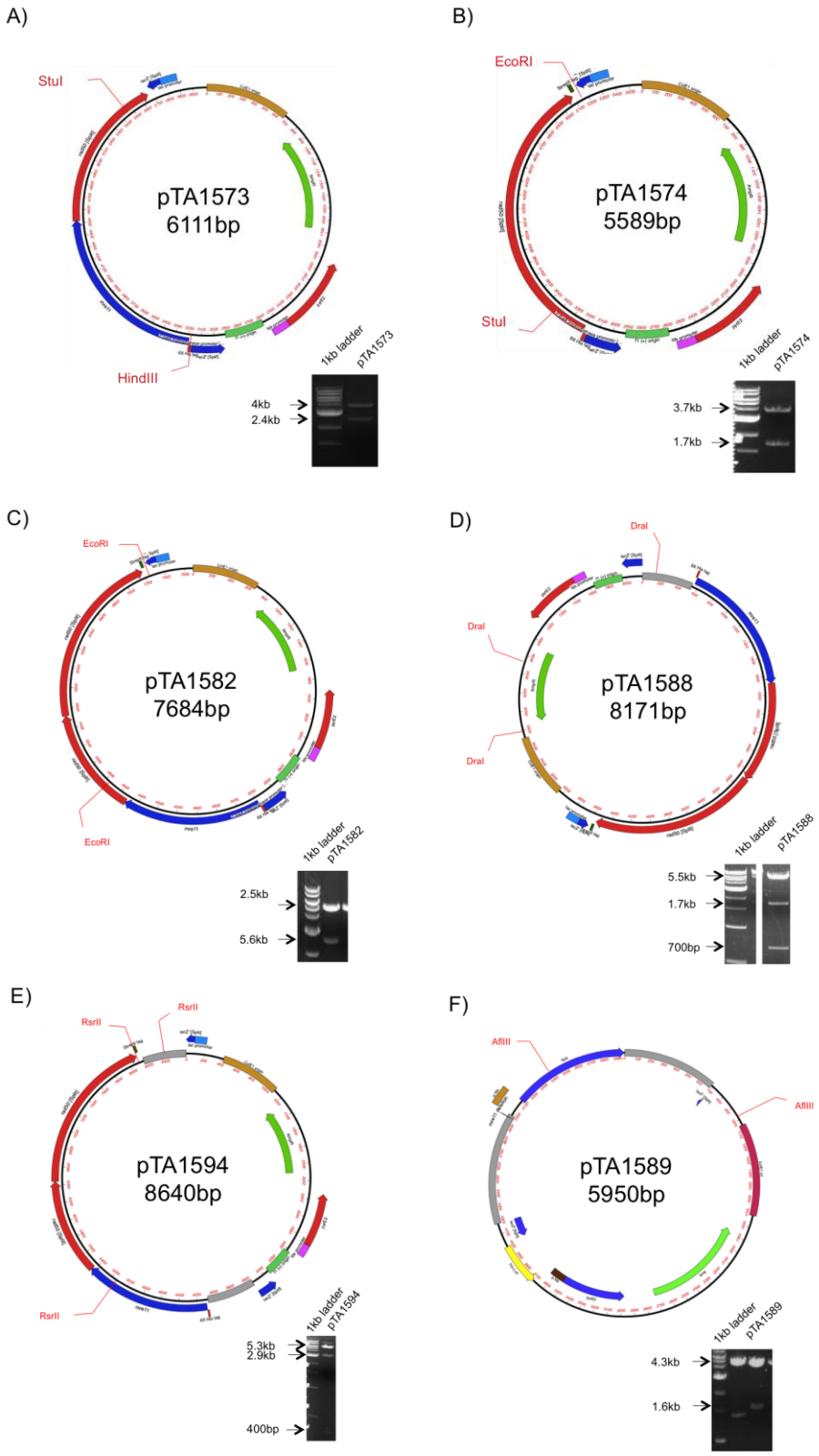

Figure 3.7. **Conformation of plasmid constructs by restriction digests. (A)** pTA1573 cut with HindIII & StuI to give 4kb and 2.4kb products. **(B)** pTA1574 cut with EcoRI & StuI to give 3.7kb &1.7kb products. **(C)** pTA1582 cut with EcoRI to give 5kb & 2.5kb products. **(D)** pTA1588 cut with DraI to give 5.5kb, 1.7kb & 700bp products. **(E)** pTA1594 cut with RsrII to give 5kb, 3kb & 400bp products. **(F)** pTA1589 cut with AflII to give 4.3kb & 1.6kb products.

3.2. Strain Construction

Several different *H. volcanii* strains were used in this study.

H115 is derived from the standard wild-type laboratory strain H26 that was obtained from the wild-type isolate DS2 by two steps: deletion of *pyrE2* (uracil biosynthesis) and curing if plasmid pHV2 (Allers *et al.* 2004; Wendoloski *et al.* 2001).

H202, H203 and H204 are derived from H115 and are deleted for *rad50, mre11 and mre11rad50* respectfully. These strains were used to observe how *mre11-rad50* affects survival rates following UV-irradiation (Delmas *et al.* 2009). They will be used to repeat these assays and study the effect of 4NQO and MMC on survival rates.

H2047 was derived from H1611, a strain deleted for *hdrB.* Linear transformation of *hdrB* into H1611 generated H2047. This strain was transformed with pTA1589 to delete *mre11rad50* from the *H. volcanii* genome. H1611 was derived from H1424, used for improved protein overexpression and purification (Stroud *et al.* 2012). H1424 was derived from H1209 (Allers *et al.* 2010).

3.2.1. Strains Containing Episomal Plasmids

Strains containing episomal plasmids were confirmed by selection on appropriate media depending on the genotype of the transformed strain and the markers present on the plasmid.

3.2.2. Gene Deletions

A pop-in / pop-out gene knock-out system for *H.volcanii* that utilises a *pyrE2* gene has been developed (Bitan-Banin et al. 2003). Orotate phosphoribosyl transferase (OPRTase) is encoded on *pyrE2* and is involved in the final step of uracil biosynthesis. Δ*pyrE2 H. volcanii* strains are transformed by using a plasmid containing a *pyrE2* marker with the flanking sequences of the gene targeted for deletion / replacement. Strains will become prototrophic for uracil once crossover occurs at the regions of homology between the deletion / replacement construct and the wild type gene (*ura+,* pop-in) (Fig. 3.8). These strains are selected for on Hv-Ca media, which lacks uracil.

A second crossover event may then occur on the chromosome at regions of homology between the newly integrated construct and the wild type gene. This results in the loss of *pyrE2* from the chromosome (*ura-,* pop-out) (Fig. 3.8). By using 5-flouroorotic acid (5-FOA), Δ*pyrE2* strains can be selected for since ura+ strains convert 5-FOA into the toxic compound 5-flourouracil, which inhibits translation. 5-FOA resistance and uracil auxotrophy is seen in *pyrE2* mutants.

A strain will either be restored to the wild-type or converted to the deletion / replacement depending on the orientation of the second crossover event relative to the first. However *H. volcanii* posses up to 20 copies of their chromosome so stains may be meridiploid, containing a mixture of mutant and wild-type alleles. Southern blotting or colony hybridization is therefore necessary to test for the presence or absence of a gene of interest.

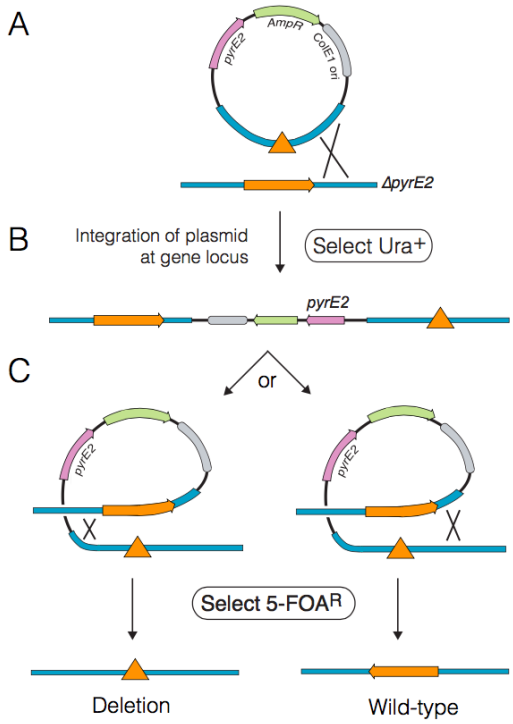

Figure 3.8: **Gene deletion by pop-in / pop-out. (A)** Δ*pyrE2* strains are transformed with a plasmid containing the flanking regions of the gene to be deleted and a *pyrE2* marker. In this example, crossover occurs at the downstream region of homology. **(B)** Pop-ins are selected by their ability to grow on media lacking uracil. **(C)** Recombination between the regions of homology on the chromosome at either upstream (left) or downstream (right) results in loss of the plasmid (and *pyrE2*). - selected for by plating on 5-FOA. The resulting gene locus will be deletion or a wild-type.

Deletion of mre11rad50

H2047 was transformed with pTA1589 to generate the pop-in strain H2109 (Δ*mre11rad50*::*trpA*+ deletion construct*)* (Fig. 3.9). Cultures were grown as previously described and plated onto Hv-Ca + 5-FOA to select for pop-outs. Slow growing candidate colonies were patched out and a colony lift performed. A radiolabelled 798bp EcoRI-StuI fragment of *mre11rad50* from pTA42 was used to probe the colony lift (Fig. 3.10). Colony PCR was also performed to confirm the deletion in strain H2110.

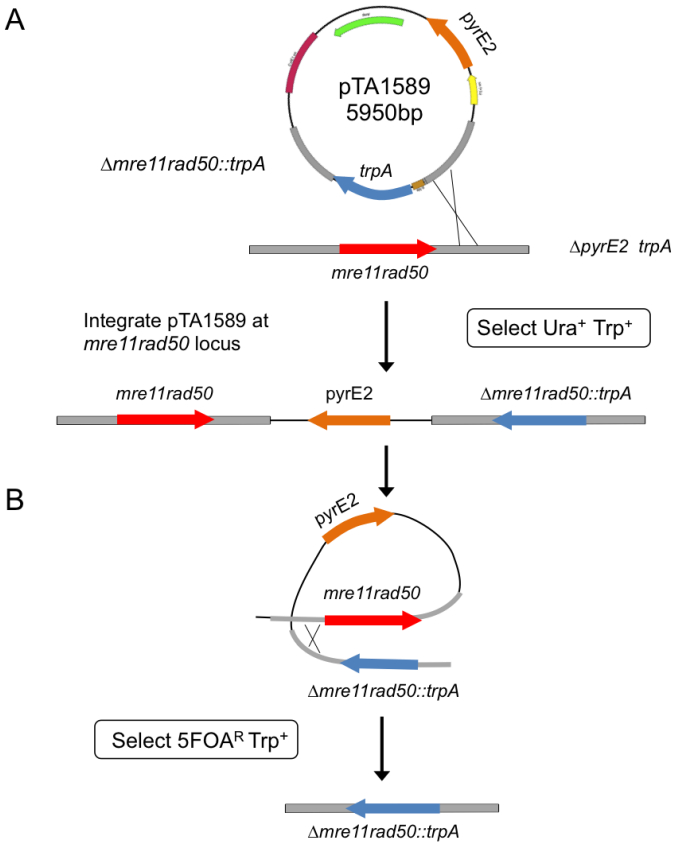

Figure 3.9: ***mre11rad50* gene deletion with trpA selection. (A)** A Δ*pyrE2* Δ*trpA* strain transformed with pTA1589, a deletion construct containing a *trpA* marked *mre11rad50* deletion and *pyrE2* marker. Pop-ins are selected by their ability to grow on media lacking uracil and tryptophan **(B)** If recombination occurs upstream between the regions of homology on the chromosome, the plasmid will be lost. Pop-outs containing *trpA* marked deletion construct are selected for by plating on 5-FOA.

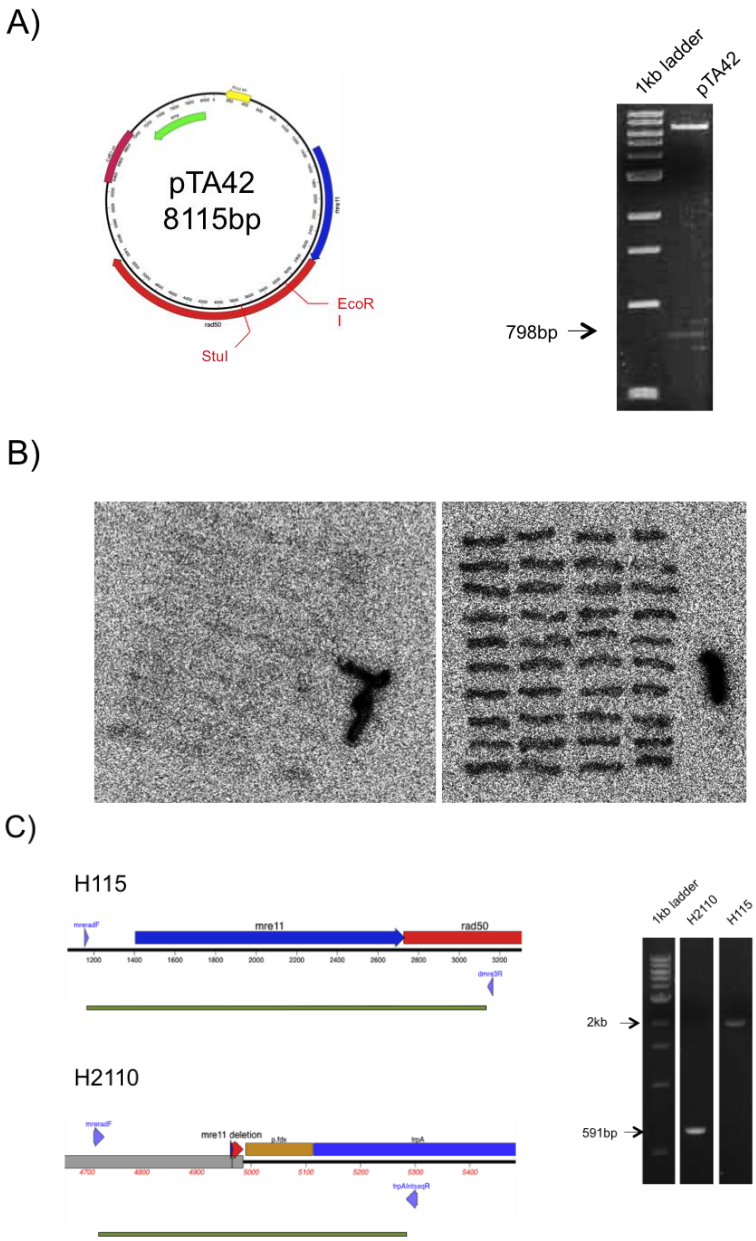

Figure 3.10. **Colony Hybridisation (A)** pTA42 cut with EcoRI & StuI to obtain798bp fragment to hybridise with native *mre11-rad50.* **(B)** Candidate colonies were screened with radiolabelled probe. Colonies that failed to hybridise were Δ*mre11rad50,* left of each set of patches is the *wild-type* strain H115. **(C)** Colony PCR was performed on H2110 using mreradF & trpAintseqR to give a 591bp fragment. PCR was performed on the wild-type strain H115 using mreradF & dmre3R to give a 2kb fragment.

3.2.3. Gene Replacements

Gene replacements were performed in the same manner as gene deletions. Replacement plasmids contained the gene of interest between flanking regions of homology.

Replacement of Mre11-Rad50

H2110 was transformed with pTA1594 (His_6/StrepII-tagged Mre11Rad50) to generate the pop-in strain H2238 (Fig. 3.11). Cultures were grown and plated onto Hv-Ca +5-FOA to select for pop-outs. To confirm the crossover between pTA1594 and the chromosome, colonies were patched out on trp+ and trp- media. The same colonies exhibited growth on trp+ media but very little growth on trp- (Fig. 3.12). This demonstrates that the strain no longer contains the *trpA* gene, since cells will not survive if they cannot synthesize tryptophan. Both crossover events must therefore have been successful. To confirm the replacement on *wild-type mre11-rad50* with His_6/StrepII-tagged *mre11rad50,* colony PCR was performed (Fig 3.13).

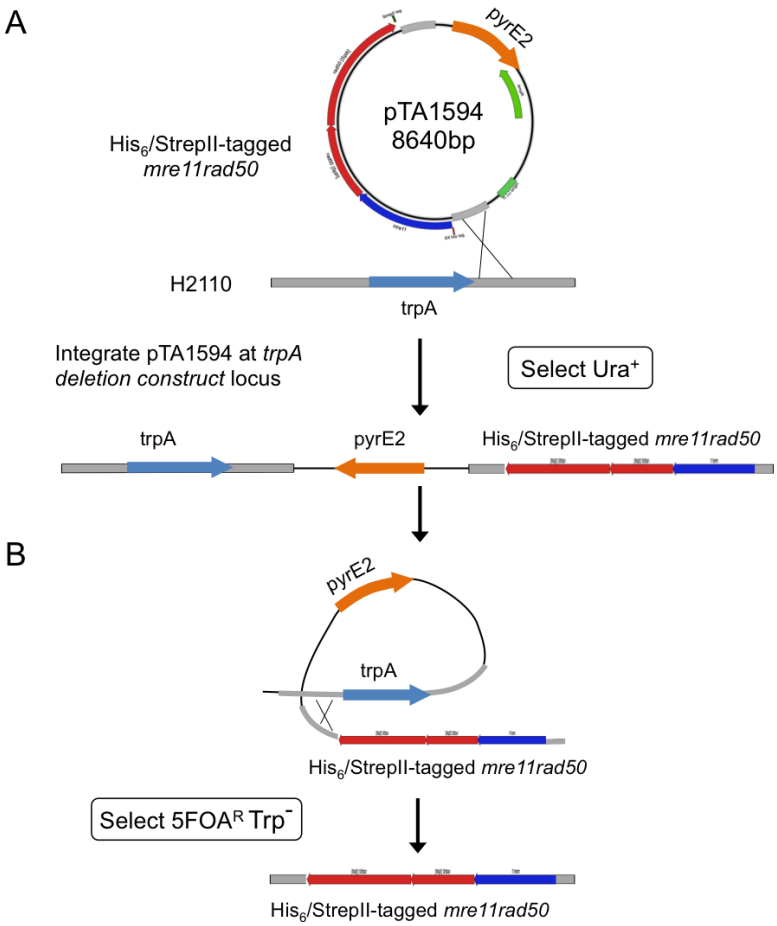

Figure 3.11: **Replacement of trpA-marked deletion construct with His_6/StrepII-tagged *mre11rad50*. (A)** H2110 (Δ*pyrE2)* transformed with pTA1594, containing His_6/StrepII-tagged *mre11rad50* and *pyrE2* marker. Pop-ins are selected by their ability to grow on media lacking uracil. **(B)** If recombination occurs upstream of *trpA*, between the regions of homology on the chromosome, the plasmid will be lost. Pop-outs containing *trpA*-marked deletion construct are selected for by plating on 5-FOA. Further selection on trp+/trp- media to check for presence of *trpA*.

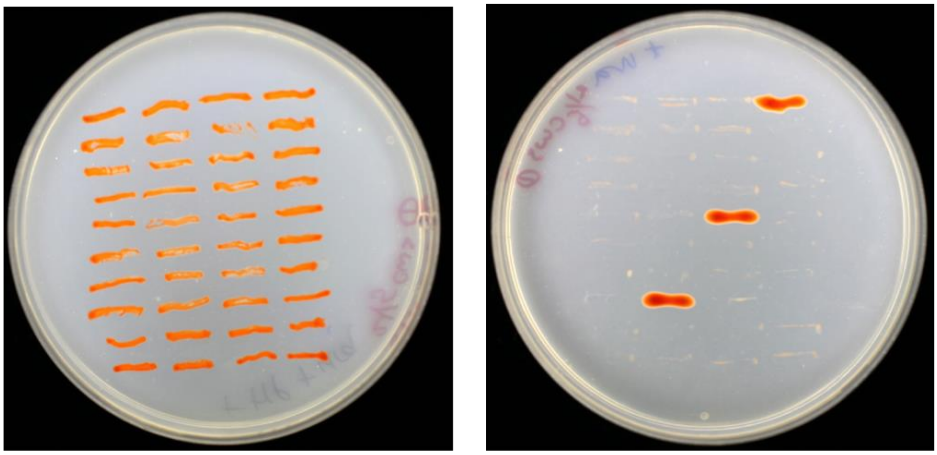

Figure 3.12. **H2239 patched on trp+ & trp- media.** Patched colonies on trp- media (right) showed almost no growth indicating that crossover between pTA1594 (His_6/StrepII-tagged Mre11Rad50) upstream of the *trp*A has occurred in strain H2239.

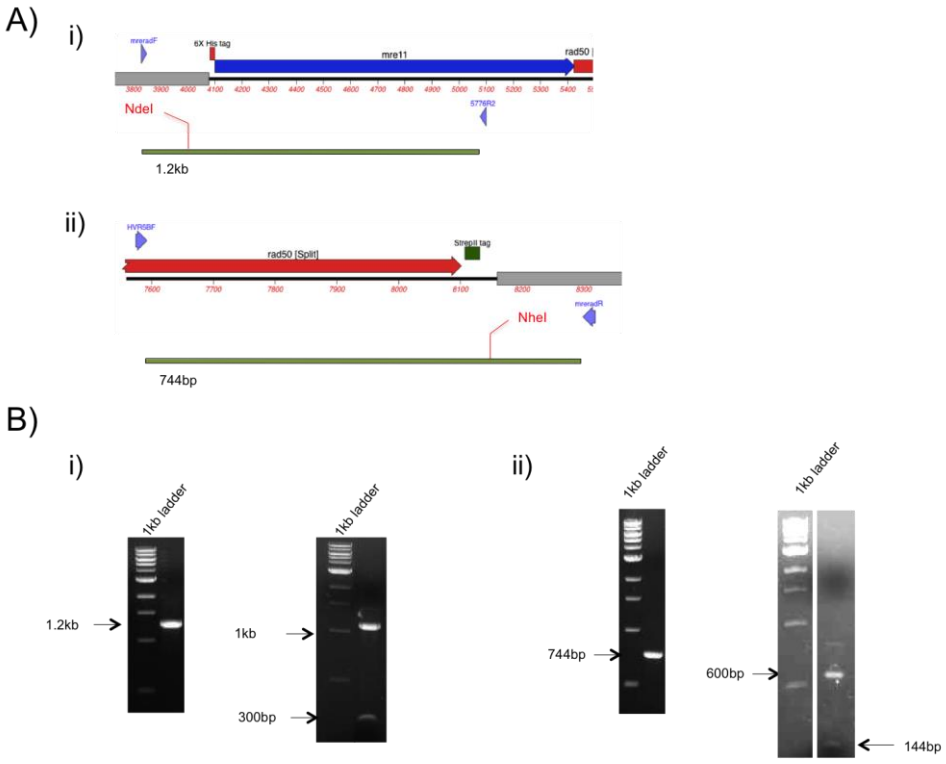

Figure 3.13. **Confirmation of strain H2239 by PCR & Digest. (A)** To confirm the pop-out strain H2239, Colony PCR was used to amplify upstream and downstream fragments of Mre11-Rad50. (i) MreradF & 5776R2 generated a 1.3kb product (upstream). (ii) HVR5BF & mreradR generate a 744bp fragment **(B)** For further confirmation of H2239 restriction digests were performed on these PCR products. (i) Upstream fragment was digested with NdeI to give 300bp and 1kb products. (ii) Downstream fragment was digested with NheI to give 600bp and 144bp products.

Chapter 4: Characterisation of Δ*mre11-rad50*

4.1. Background

4.1.1. Δ*mre11-rad50 H. volcanii*

H. volcanii Δ*mre11-rad50* strains show increased resistance to DNA damage (Delmas *et al.* 2009). When DSBs are induced, Mre11-Rad50 is believed to restrain HR to allow other repair pathways to operate. In *H. volcanii,* which is polyploid, this method of repair may benefit the organism by preventing DNA ends engaging with multiple partners. However when Mre11-Rad50 is not present, there is no mechanism preventing HR from operating. HR is exclusively used to repair DSBs, causing *H. volcanii* to become hyper-resistant to DNA damage. However adopting this method of repair leads to slower recovery, presumably due to the processing time needed for HR to operate (Delmas *et al.* 2009).

Survival following UV-irradiation

UV light can induce lesions in DNA, which result in single and double-strand DNA breaks (Goosen & Moolenaar 2008). These breaks may occur when Cyclobutane pyrimidine dimers (CPDs) and (6-4) photoproducts distort the DNA backbone and block replication forks. *H. volcanii* WT and Δ*mre11-rad50* strains have been treated with UV light and survival fractions calculated (Delmas *et al.* 2009). H202 (Δ*rad50*), H203 (Δ*mre11*) and H204 (Δ*mre11rad50*) all exhibited increased resistance to DNA damage by UV light compared to the wild-type strain H115 (Fig 4.1).

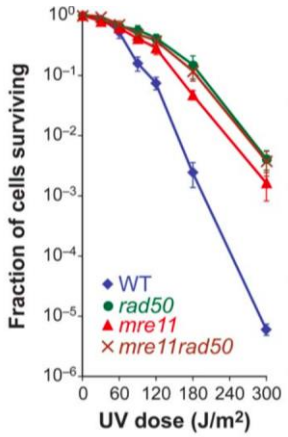

Figure 4.1: **UV survival frequency for Δ*rad50,* Δ*mre11* & Δ*mre11rad50* strains.** Mutants show increased resistance to DNA damage by UV-irradiation (Delmas *et al.* 2009)

4.2. Aims

The aims of this chapter are to:

- Confirm data obtained by Stéphane Delmas and Thorsten Allers (Delmas et al. 2009). Studying how deleting *mre11-rad50* from *H. volcanii* affects survival rates when cells are exposed to UV light.
- Study the effect of MMC, 4NQO and UV-irradiation on the same strains used by Delmas et al.
- Study effect of 4NQO, MMC and UV light on *mre11-rad50* deletion strain H2110.
- Use Data from survival curves to obtain a drug concentration giving a 90% survival rate.

4.3. Results

4.3.1 Δ*mre11-rad50* Genetic Analysis

Survival following UV-irradiation

To test the ability of Δ*mre11-rad50* strains to repair UV-induced lesion, WT and mutant strains were treated with UV light and survival fractions calculated. Strains H115, H202, H203 and H204 were cultured with the addition of H2110 (Δ*mre11-rad50),* which was derived from H2047. Strains were grown to mid-exponential phase spotted out over a range of dilutions onto YPC media. Separate plates were irradiated in a UV light box for 60s, 90s, 120s and 180s.

All strains displayed the same phenotype seen in the previous assays (Delmas et al. 2009). Mutant strains H202, H203 and H204 exhibited an increased rate of survival compared to wild-type H115, indicating that they are more resistant to DNA damage by UV-irradiation. H2110 also showed significantly greater survival than H115, similar to H204 (Fig. 4.2).

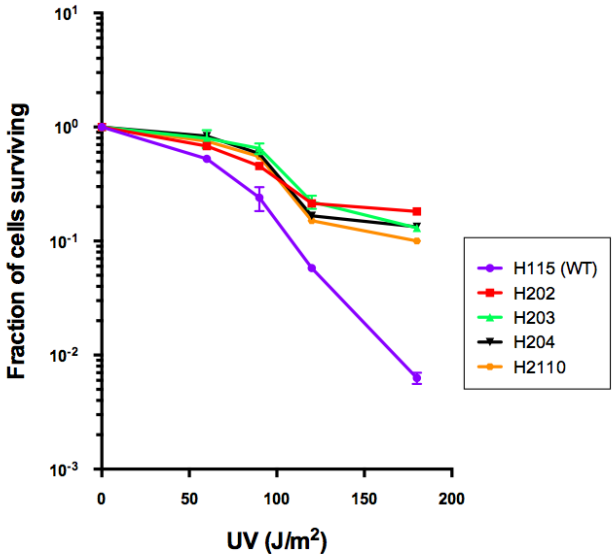

Figure 4.2. **UV survival frequency for Δ*rad50*, Δ*mre11* & Δ*mre11rad50* strains.** Mutant strains display enhanced survival over *wild-type,* indicating increased resistance to DNA damage by UV-irradiation. Survival fraction is calculated relative to an un-treated control. Each data point is generated as an average of at least 2 independent trials. Standard error is shown. Plotted using GraphPad Prism 6.

Survival following 4NQO incubation

The carcinogen 4-nitroquinoline 1-oxide (4NQO[2]) has been shown to cause DSBs (Andoh & Ide 1972). This chemical compound will be incubated with large-scale liquid cultures when protein purification assays are performed to induce DSBs in *H. volcanii*. UV-irradiation cannot be used to induce damage in such large-scale liquid cultures needed for protein preparation.

Mutant strains H115, H202, H203, H204 and H2110 were grown to mid-exponential phase and incubated with increasing concentrations of 4NQO (0.2µg/ml, 0.42µg/ml, 062µg/ml and 0.82µg/ml) and plated out over a range of dilutions. As expected, the survival fractions of the mutant strains were greater than the wild-type. These findings display similarity to the results from UV-irradiation assays performed in this study and in previous studies (Delmas *et al.* 2009). H202, H203, H204 and H2110 showed an increased resistance to DNA damage caused by 4NQO when compared with WT H115 (Figure 4.3).

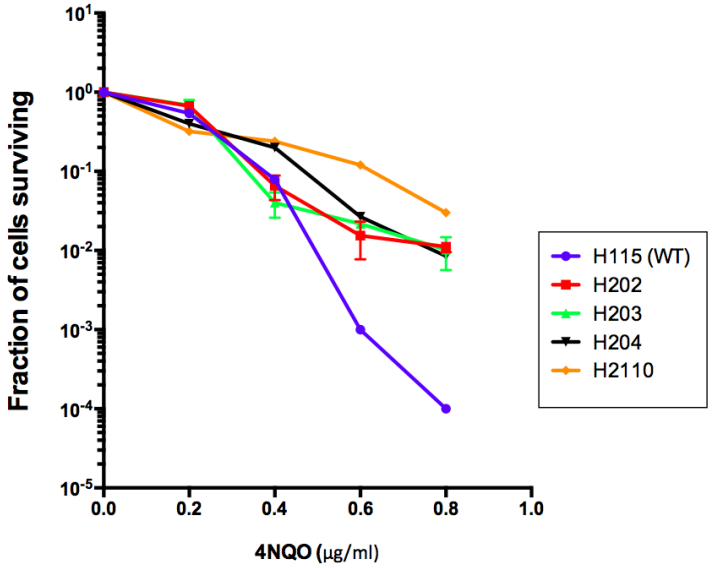

Figure 4.3. **Survival frequency for Δ*rad50*, Δ*mre11* & Δ*mre11rad50* strains following treatment with 4NQO.** Mutant strains display enhanced survival over wild-type, indicating increased resistance to DNA damage by UV-irradiation. Survival fraction is calculated relative to an un-treated control. Each data point is generated as an average of at least 2 independent trials. Standard error is shown. Plotted using GraphPad Prism 6.

The survival curves from the 4NQO were performed to determine the point at which colonies exhibited a 90% survival rate for the WT. This step was needed to confirm the concentration of 4NQO required for incubation with *H. volcanii* prior to protein purification on His_6/StrepII gravity columns.

Survival following MMC treatment

Mitomycin C (MMC) is a DNA inter-strand crosslinking agent that can result in stalled replication forks if HR or NER do not repair the crosslink itself. Mre11-Rad50 is not directly involved in crosslink repair but is perhaps indirectly involved. DSBs could be induced following replication fork collapse, so Mre11-Rad50 may be recruited to initiate repair by HR.

Strains H115, H202, H203, H204 and H2110 were grown to mid-exponential phase and plated onto media containing 0.01, 0.015, 0.02, 0.025, 0.03µg/ml MMC or no MMC as a control (Fig. 4.4). All mutant strains were less resistant to the damage than WT. This demonstrates that *mre11rad50* is involved in the repair of DNA crosslinks.

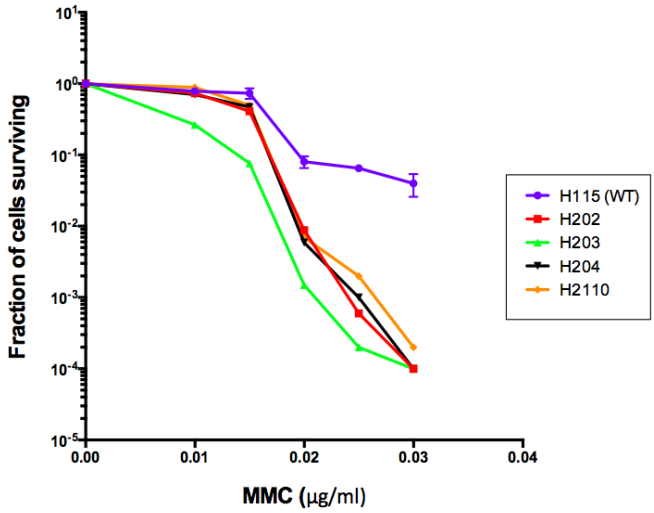

Figure 4.4. **Survival frequency for Δ*rad50*, Δ*mre11* & Δ*mre11rad50* strains following treatment with MMC.** *Wild-type* strains display enhanced survival over mutant strains, indicating Mre11rad50 is involved in the repair of inter-strand crosslinks. Survival fraction is calculated relative to an un-treated control. Each data point is generated as an average of at least 2 independent trials. Standard error is shown. Plotted using GraphPad Prism 6.

4. 4 Discussion

Δmre11-rad50 strains are more resistant to DNA damage than the wild-type

DNA damage assays performed in this study were carried out to support data from previous experiments where similar assays were performed (Delmas *et al.* 2009). Previous assays utilised UV-irradiation, phleomycin, MMS and γ radiation to induce DNA damage. In this study UV-irradiation and 4QNO were used to induce double strand breaks in *H. volcanii*.

The results obtained from UV-irradiation and 4NQO DNA damage assays showed that Δ*rad50*, Δ*mre11* and Δ*mre11rad50* strains were more resistant to the damage than the wild-type strain. The survival frequency curves calculated from the assays show a similar trend to the curves generated in previous studies in all four strains (Delmas *et al.* 2009). The Δ*mre11rad50* strain H2110 generated for this study displayed similar resistance to DNA damage as H204 as expected (Δ*mre11rad50*).

The data from this study support the conclusions drawn from past studies; that Δ*mre11rad50* strains are more resistant to DNA damage than wild-type.

It has been proposed that if Mre11-Rad50 is not present in *H. volcanii,* an alternative to repair pathway to HR cannot be used. The damage resistance is thought to be due to the unrestricted use of HR to repair DSBs caused by the induced DNA damage. Exclusively using HR as a repair mechanism would lead to higher levels of damage being repaired (Delmas *et al.* 2009).

Δmre11-rad50 strains recover more slowly following damage

The sole use of HR to repair DSBs appears to decrease the recovery rate of Δ*mre11rad50 H. volcanii*. Colonies formed by surviving Δ*mre11rad50* cells following DNA damage are smaller than *wild-type* cells (Delmas *et al.* 2009). Also *wild-type* cell have a significantly faster recovery following damage when compared with Δ*mre11rad50* cells in growth competition assays. The decreased recovery rate in Δ*mre11rad50 H. volcanii* may be a result of the slower repair of DSBs by HR. Meanwhile WT cells possess a long-term advantage by adopting a different repair strategy, which is faster than HR. *Halobacterium sp.* NRC-1 Δ*mre11rad50* mutants also display an extensive delay in repair of DSBs (Kish & DiRuggiero 2008). When the structural homolog of Mre11-Rad50 (sbcCD) is deleted in *D. radiodurans,* there is a significant delay in DSB repair (Bentchikou *et al.* 2007).

Difference of repair pathway between wild-type and mutant strains

H. volcanii Δ*mre11rad50* strains have been shown to preferentially use HR to repair DSBs, whereas *wild-type* strains almost exclusively use accurate end-joining (Delmas *et al.* 2009). A series of recombination assays using replicative plasmids revealed that Δ*mre11rad50* strains used a different DSB repair mechanism to the *wild-type* (Fig. 4.5 adapted from Delmas *et al.* 2009). In contrast, when *mre11* is deleted from *S. cerevisiae,* HR between chromosome and plasmid is reduced (Lewis *et al.* 2004). *S. cerevisiae* further differs from *H. volcanii* as HR is stimulated in the presence of DSBs rather than restrained (Orr-Weaver *et al.* 1981).

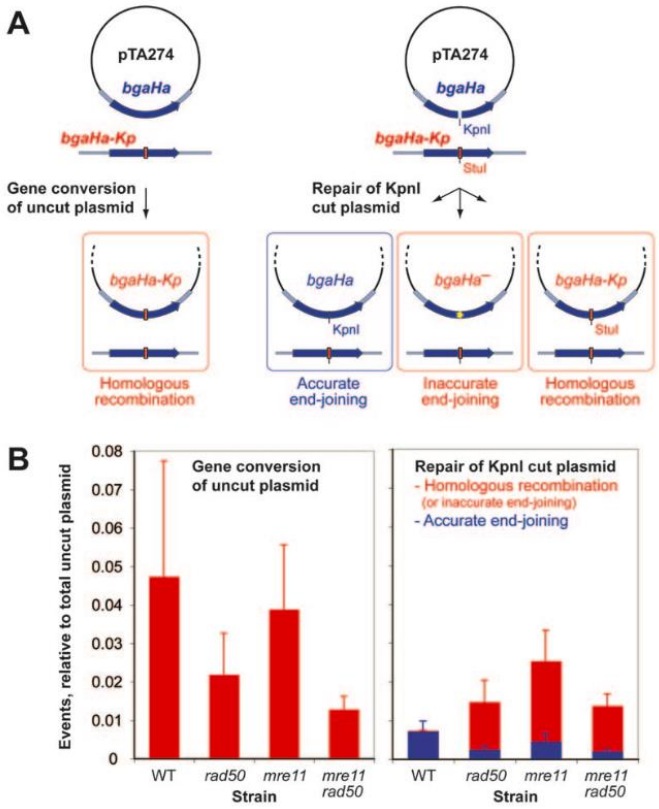

Figure 4.5**. Δ*mre11-rad50* strains of *H. volcanii* show elevated levels of HR relative to wild-type.** **(A)** pTA274 carries 3kb fragment with *bgaHa* beta-galactosidase gene. Chromosomal *bgaHa* allele contains a StuI site. Uncut plasmid may be gene converted by the chromosomal bgaHa-Kp allele, while plasmid cut at the KpnI site may be repaired in three ways: accurate end joining, inaccurate end-joining or homologous recombination. **(B)** Wild-type (H115), *rad50* (H202), *mre11* (H203) and *mre11rad50* (H204) were transformed with either uncut (left) or KpnI-cut pTA274 (right). Wild-type favours end-joining whilst mutant strains use HR (Adapted from Delmas *et al.* 2009)

MMC survival fractions

In contrast to the trends seen in UV-irradiation and 4NQO assays, the MMC survival fractions indicated that the wild-type strain was more resistant to DNA damage than *mre11, rad50* and *mre11rad50* mutant strains. This suggests that Mre11-Rad50 is involved in the repair of MMC-induced damage in *H. volcanii.* At the time the experiment was carried out this result had never been seen before, however recent data has been published displaying the same results (Giroux *et al.* 2015). The increased sensitivity of the mutant strains to MMC may be due to a failure to prevent replication fork collapse. Since Mre11-Rad50 helps to maintain the stability of stalled

replication forks in eukaryotes (Tittel-Elmer *et al.* 2009), the complex may perform the same role in *H. volcanii* if stalling occurs at DNA crosslinks induced by MMC.

4NQO survival fractions

The concentration of 4NQO required to give 90% survival was determined to prevent excessive cell death of in liquid cultures *H. volcanii* following incubation with this compound. From the survival curves calculated 0.2μg/ml 4NQO appears to give a survival fraction of ~ 90% after one hour of incubation. This concentration will be used in large-scale liquid cultures (~2l). This step will induce DSBs in the *H. volcanii* genome. When Mre11-Rad50 is purified from His_6/StrepII gravity columns, proteins linked to the complex during DSB repair could also be purified.

Chapter 5: Biochemical analysis of Mre11-Rad50

5. 1. Background

5. 1. 1. Halophilic Proteins

Protein purification

Under conditions of low salt, halophilic proteins are usually insoluble and can aggregate and misfold. They are therefore difficult to express in heterologous hosts (e.g. *E. coli*) and often require recovery from inclusion bodies followed by denaturing and refolding under high salt conditions (Connaris et al. 1999). This can only be achieved with well-characterised proteins when correct folding can be confirmed by a functionality assay.

Purification of halophilic proteins expressed in E. coli

H. volcanii dihydrofolate reductase has been expressed in *E. coli* (Blecher et al. 1993). The insoluble protein required denaturing and reconstitution using guanidine hydrochloride followed by purification. This was achieved in 1M NaCl using both ammonium sulphate precipitation and ion exchange chromatography.

His_6-tagged RPA3 (ssDNA binding protein in *H. volcanii*) has been expressed in *E. coli* (Winter et al. 2012). Protein expression was induced and cell pellets were resuspended in buffer containing 1M NaCl. Purification was achieved using a combination of ammonium sulphate precipitation, metal affinity chromatography and size exclusion chromatography.

Purification of halophilic proteins expressed natively in H. volcanii

Dilhydrolipoamide dehydrogenase has been expressed in *H. volcanii* (Jolley et al. 1996). Hydroxylapatite chromatography was used to purify the protein. Positively charged calcium ions and negatively charged phosphate ions interact non-specifically with proteins (Cummings et al. 2009). Using phosphate-containing elution buffer, proteins are eluted at different points depending on their properties.

HMG-CoA (leucine biosynthesis protein) has been expressed natively in *H. volcanii* (Bischoff and Rodwell 1996). It was purified using size exclusion chromatography, ammonium sulphate precipitation and hydroxyapatite column.

More recently the 20S proteasome from *H. volcanii* was expressed and purified using His_6/StrepII tags (Humbard et al. 2009). The α1-subunit and ß-subunit were tagged with His_6 and StrepII respectively. This enabled the purification of the whole protein complex using a metal affinity column followed by a StrepTactin column. This was the approach used to purify proteins in this study.

5. 1. 2 Strains for protein overexpression

H. volcanii strains developed for native protein expression were used in this study. H2047 (ΔpyrE2, Δmrr, Nph-pitA, cdc48d-Ct) was originally derived from H1424 (ΔpyrE2, ΔhdrB, Δmrr, Nph-pitA, cdc48d-Ct). H1424 was derived from H1209 (ΔpyrE2, ΔhdrB, Δmrr, Nph-pitA), a strain deleted for the restriction endonuclease Mrr.

Deletion of Restriction Endonuclease Mrr

Mrr is encoded by *H. volcanii* and cuts methylated 5'-GATC-3' sequences. Methylation of 5'-GATC-3' is carried out by a Dam methylase in *E. coli* so plasmid DNA must be passaged through *dam- E. coli* prior to transformation into *H. volcanii* (Holmes et al. 1991). *Dam- E.coli* cannot be used to generate plasmids directly. The absence of Dam-methylase results in an inability to differentiate between parental and newly synthesised daughter strands during mismatch-repair (Glickman et al. 1978, Li 2008). To avoid passage of *dam+* plasmids through *dam- E. coli* strains deleted for *mrr* have been developed (Allers et al. 2010). Because certain plasmids contain genes that are toxic to *E. coli,* they must be constructed directly in *H. volcanii* deleted for *mrr.*

Replacement of pitA

The protein PitA is unique to *H. volcanii* and consists of two distinct domains; a chlorite dismutase-like N-terminal domain and an antibiotic biosynthesis monooxygenase-like C-terminal domain (Bab-Dinitz et al. 2006). A histidine-rich

linker links these domains. This causes PitA to be a major co-contaminant when purifying His-tagged proteins using metal affinity chromatography (Bab-Dinitz et al. 2006, Humbard et al. 2009). However PitA is essential to *H. volcanii* so cannot be deleted (Allers et al. 2010). Native *H. volcanii pitA* has been replaced with *pitA* from *Natronomonas pharaonis, which* contains no histidine-rich linker between the two domains.

Replacement of cdc48d

Cdc48d is a putative AAA+ ATPase. It shares homology with eukaryotic Cdc48, a ubiquitin-dependant chaperone involved in protein degradation and with bacterial FtsH, a Zn^{2+} metalloprotease that degraded certain short-lived protein (Meyer & Popp 2008; Ito & Akiyama 2005). In *H. volcanii,* Cdc48d contains a histidine-rich C-terminus that enables the protein to bind to metal affinity columns.

Cdc48d is essential in *H. volcanii* and cannot be delete from its genome (Allers *et al.* 2010). Attempts were made to replace the protein. Firstly with Cdc48d from *H. salinarum* (H1333), which still bound to the metal affinity column. Secondly with Cdc48d from *H. marismortui* (H1405), which eliminated contamination but adversely, affected cell growth. Deletion of histidine-rich C-terminal was later carried out to generate the H1424 (Stroud *et al.* 2012). This strain showed no growth defect and did not contaminate metal affinity columns.

5. 1. 3. Development of methods

Improvement of Previous Methods

Methods employed in this chapter were developed from previous techniques, which have been used successfully to purify proteins expressed natively in *H. volcanii.* These techniques utilised His_6 –tagged proteins to investigate *in vivo* protein:protein interaction (Allers *et al.* 2010; Stroud *et al.* 2012; Wardell 2013). Methods used previously produced a large number of histidine-rich contaminants, which makes protein bands problematic to identify. If a protein of interest happens to be the same size of a histidine-rich contaminant, it may not be analysed. Also histidine-rich proteins may be dismissed as contaminants despite revealing a genuine interaction.

Due to these restrictions, an alternative protocol was used which employed a StrepII-tag for purification, which had less contaminants on the purification resin. This method has been shown to function in high salt and has been successfully used to purify proteins natively from *H. volcanii* (Humbard *et al.* 2009). StrepII-tags are only 8 amino acids long and bind with high specificity to StrepTactin columns with a low level of non-specific binding. However, StrepII-tags give a lower protein yield than His_6 –tags, therefore protein samples will be precipitated with TCA.

5. 2. Aims

The aims of this chapter are to:

- Express His_6/StrepII-tagged Mre11-Rad50 natively in *H. volcanii* and identify proteins that co-purify with the complex. This will provide an insight into any unidentified proteins involved in DSB repair give further insight into the role Mre11-Rad50 plays in this process.

5. 3. Results

In *H. volcanii,* Mre11-Rad50 has been proposed to temporarily restrain DSB repair by HR to allow repair by other pathways (Delmas et al. 2009). It is thought that Mre11-Rad50 directly prevents HR (possibly through blocking the formation of RadA filaments) rather than actively promoting a different pathway such as MMEJ. This mechanism is thought to be advantageous to the polyploid organism. If HR is used exclusively to repair DSBs, DNA ends risk engaging with multiple partners and creating chromosome concatemers. The time needed for DSB repair by HR may also incur further cost to *H volcanii.*

The protein interactions of Mre11-Rad50 are currently unknown in *H. volcanii*. Identification of these proteins will help elucidate the role of Mre11-Rad50 during DSB repair and may give insight into how HR is restrained.

5. 3. 1. Protein Purification

Metal Affinity Chromatography

His_6/StrepII-tagged proteins were purified from cell lysate by metal affinity chromatography. Gravity columns were packed with charged Sepharose beads. These were chosen for their ease of use for small-scale purifications. The His_6 gravity column used Ni^{2+}-charged beads to generate the highest protein yield in conditions of >1M NaCl (Allers et al. 2010). Numerous histidine-rich contaminants bind to His_6 gravity columns (Fig. 5.4); the use of StrepTactin columns alleviated this problem.

Concentration of Proteins

Vivaspin ultrafiltration spin columns with an appropriate molecular weight cut-off were used to concentrate protein samples.

Purification of His_6/StrepII –tagged Mre11-Rad50

The Mre11-Rad50 complex was purified from H2239, a strain containing the plasmid pTA1594. Rad50 was seen to co-purify with Mre11 on SDS-PAGE gel from both the His_6 and StrepII columns (Fig. 5.1, Fig. 5.2). A number of additional bands can be seen in elutions from the His_6 column (Fig. 5.1). Some of these products are likely to be histidine-rich contaminants. Many of these bands are not seen in elution samples from the StrepII column (Fig. 5.2). However several additional bands are present in elutions and vivaspin samples from both columns.

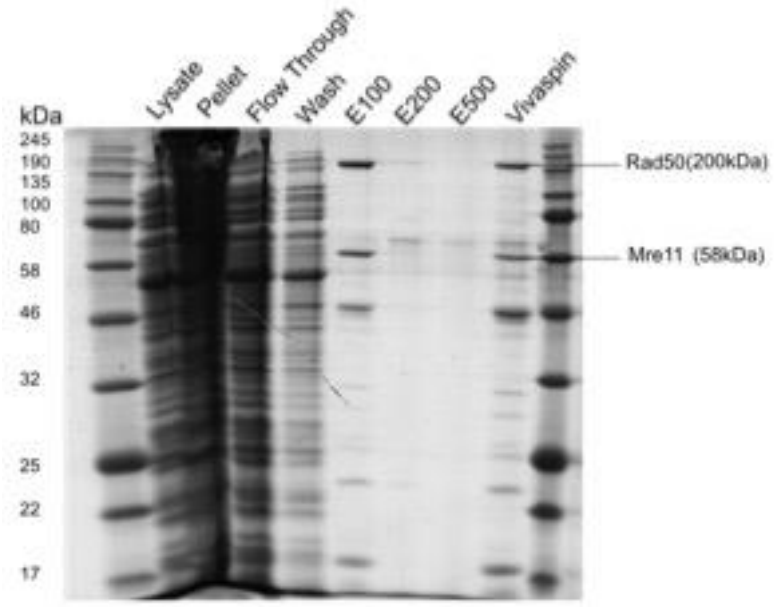

Figure 5.1: **Purification of His-tag**. His_6/StrepII-tagged Mre11-Rad50 was expressed and purified from H2239 by metal affinity chromatography using a step-gradient of elution buffer containing imidazole (E refers to the imidazole concentration in mM). Vivaspin sample obtained by pooling together elution samples. Bands were identified by mass spectrometry (performed by Susan Liddell, University of Nottingham).

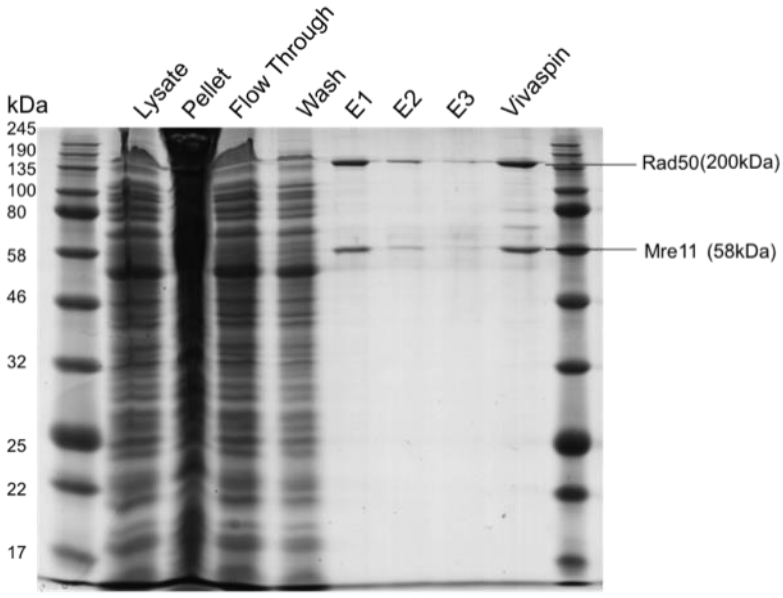

Figure 5.2: **Purification of Strep-tag**. His6/StrepII-tagged Mre11-Rad50 was expressed and purified from H2239 by Streptactin affinity column. E1 was eluted in 0.8ml elution buffer, E2 with 1.4ml and E3 with 0.8ml.Vivaspin sample obtained by pooling together elution samples. Bands were identified by mass spectrometry (performed by Susan Liddell, University of Nottingham).

Screening for Interacting Partners of Mre11-Rad50

To concentrate the vivaspin samples from both His_6 and StrepII columns, precipitation was carried out with DOC, TCA and acetone to make the shared bands more visible on SDS-PAGE gel (Fig. 5.3). Two bands were putatively identified as hypothetical protein HVO_2381 (46 kDa) and HVO_A0388 (17 kDa), a transcriptional regulator. A number of histidine rich contaminants have been previously identified and were used as a guide to identify these proteins (Fig. 5.4). Three additional shared bands were present in elutions from both affinity columns, which are presumably proteins interacting with Mre11-Rad50.

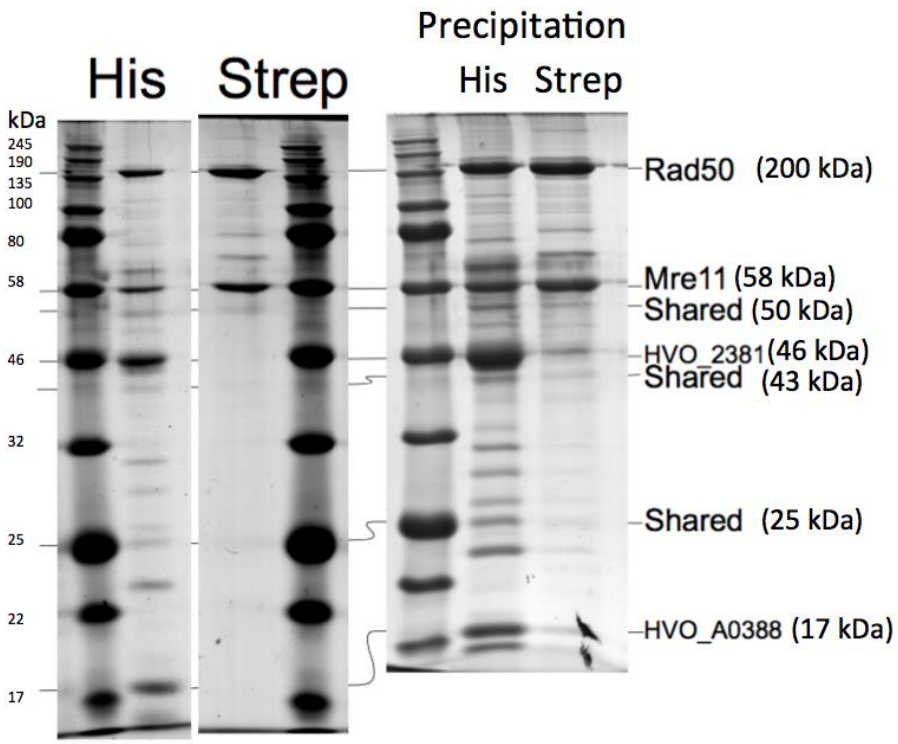

Figure 5.3: **Precipitation of samples.** Vivaspin samples from His and Strep columns cleaned up by precipitation with DOC, TCA & Acetone. Contaminants HVO_2381 and HVO_AO388 putatively identified but 3 shared proteins appeared on both the His_6 and StrepII columns. Bands were analyzed using mass spectrometry (performed by Susan Liddell, University of Nottingham) (See Appendix).

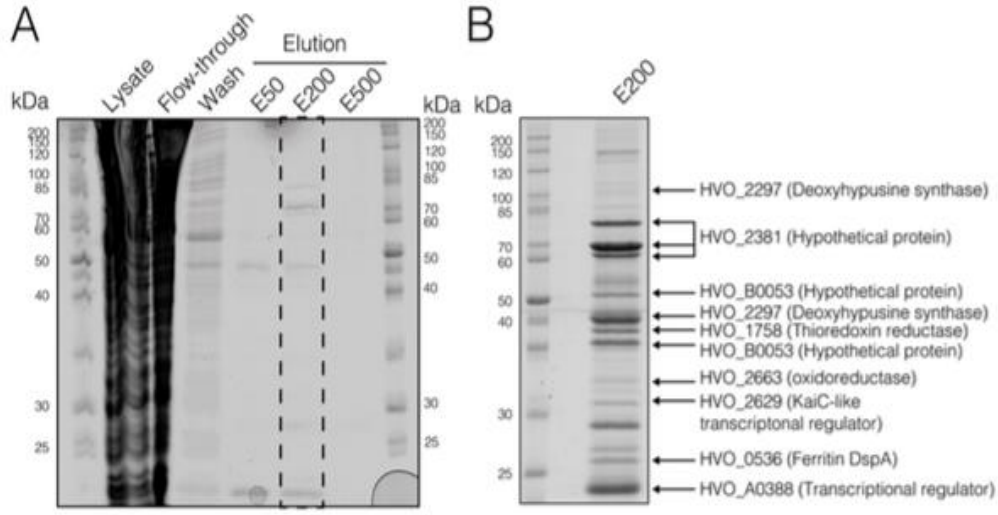

Figure 5.4: **Histidine-rich contaminating proteins in co-purification assays.** **(A)** Eluted samples after H1424 was applied to Ni^{2+} gravity column. **(B)** E200 sample was precipitated using TCA and histidine-rich contaminants identified by mass-spectrometry. (Wardell 2013)

5. 4. Discussion

Co-purification of Mre11 and Rad50

Protein purification assays show that His_6/StrepII-tagged Mre11 and Rad50 interact *in vivo* in *H. volcanii.* As the two molecules are part of a protein complex this was expected. Protein samples from cell lysate were eluted separately from His_6 and StrepII gravity columns and two strong bands (200kDa & 58kDa) were identified from both columns. These were analysed by mass spectrometry and confirmed to be Mre11 (58kDa) and Rad50 (200kDa) through comparison with other known protein sequences (See Appendix).

Proteins purifying with His_6/StrepII –tagged Mre11-Rad50

Protein purification assays and protein precipitation have highlighted a number of potential protein interactions of Mre11-Rad50 as well as two hypothetical protein interactions. The hypothetical proteins HVO_2381 and HVO_A0388 were identified putatively from both His_6 and StrepII columns. Co-purification assays performed using H1424 have revealed a number of histidine-rich contaminants, which have been analysed by mass spectrometry (Wardell 2013) and were used to identify these bands. Three additional bands were shared between both columns and were visible following

protein precipitation. These proteins (25kDa, 43kDa & 50kDa) are presumably interacting with Mre11-Rad50 under normal growth conditions. Due to time constraints, these bands could not be identified. (See appendix for mass spectrometry results received following thesis submission of proteins found to be interacting with Mre11-Rad50).

Mre11-Rad50 has been shown to interact with different proteins under various conditions. In eukaryotes RPA has been shown to interact with the complex at sites where replication forks stall (Robison *et al.* 2004).A functional interaction between Mre11, Rad50 and HerA bipolar helicase has been demonstrated *S. acidocaldarius* following gamma irradiation (Quaiser *et al.* 2008). HerA interacts with NurA which is thought to function with RadA during DNA repair. Future findings should reveal which proteins Mre11-Rad50 interact with in *H. volcanii* to repair DNA (Mass spectrometry data in appendix reveals RadA is co-purifying with Mre11-Rad50 in *H. volcanii*).

Further Analysis

The next stage in this study was to carry out the same protein purification assays under conditions of DNA-damage with 4NQO. Following overnight culturing, liquid cultures would be incubated with 0.02 µg/ml 4NQO to introduce DSBs to the *H. volcanii* genome. This would reveal whether the interactions of Mre11-Rad50 remain the same under these conditions or if new interacting partners can be identified. Analysis through mass spectrometry would be carried out on any new bands found on SDS-PAGE gel.

To stabilise the interactions of Mre11-Rad50 with other proteins, crosslinking could be implemented with 1-ethyl-3-[3-dimethylaminopropyl] carbodiimide hydrochloride (EDC). EDC is a zero-length crosslinker, which can directly conjugate carboxylates to primary amines. Direct binding between proteins is possible without EDC becoming incorporated into the final crosslink. Following incubation with 4NQO and prior to cell lysis by sonication, liquid cultures would be pelleted and resuspended in buffer A, then treated with 10Mm EDC. Samples would be sonicated and purified on His_6 and StrepII columns and the elutions run on SDS-PAGE gel.

Chapter 6: Conclusion and Future Perspectives

Mre11-Rad50 plays a crucial role in the repair of double-strand DNA breaks. The complex tethers DNA ends to prevent chromosomal rearrangements, influences DSB repair pathway choice (Delmas *et al.* 2009) and is involved during nucleoid compaction as a response to DNA damage in *H. volcanii* (Delmas *et al.* 2013). Deletion of *mre11rad50* confers hypersensitivity to DNA damage in *H. volcanii* but causes slower recovery. The unrestrained use of HR to repair DSBs is thought to cause this DNA damage resistance since Mre11-Rad50 is not present to restrain this pathway.

DNA damage assays

DNA damage assays were performed on *mre11, rad50* and *mre11rad50* mutant strains and a wild-type strain of *H. volcanii* used in previous studies (Delmas *et al.* 2009). The *mre11-rad50* deleted strain generated for this study (H2110) was compared to these strains. The assays were performed using UV-irradiation, 4NQO and MMC. The UV-irradiation and 4NQO assays showed that all mutant strains were more resistant to the damage than the wild-type. These results support the findings made in previous studies (Delmas *et al.* 2009).

The MMC assays showed that the mutant strains were less resistant to the damage than the wild-type. The mutant survival rates were significantly reduced suggesting that Mre11-Rad50 is being utilised in the repair of DNA-interstrand crosslinks. The assays should be repeated to confirm these findings.

The involvement of Mre11-Rad50 in the repair of MMC-induced damage in *H. volcanii* or any other haloarchaea had not been demonstrated prior to the assays being performed. Another group has recently published data supporting the results obtained from these assays (Giroux *et al.* 2015).

Cloning and Protein Analysis

Native *H. volcanii mre11rad50* was cloned using PCR and restriction digest to generate pTA1594, a His_6/StrepII-tagged plasmid containing *mre11rad50* and its upstream and downstream flanking regions. pTA1589, a *trpA*-marked deletion construct was also generated by restriction digest. This contained the selectable marker *trpA* and the upstream and downstream flanking regions of *mre11rad50.*

mre11-rad50 has been deleted from the *H. volcanii* genome and replaced with His_6/StrepII-tagged *mre11rad50*. This was achieved using the pop-in pop-out method of transformation to first generate the strain H2110 containing pTA1589. H2110 was then transformed with pTA1594 to replace the deletion construct with His_6/StrepII-tagged *mre11rad50.*This was expressed using the native *mre11rad50* promoter and purified from His_6 and StrepII affinity columns. This step was carried out to identify the protein interactions of Mre11-Rad50.

The identities of Mre11 and Rad50 were confirmed by mass spectrometry and the proteins were shown to co-purify on SDS-PAGE gel. A number of proteins appear to co-purify with Mre11-Rad50 but further analysis with mass spectrometry is needed to determine their identity. Future experiments need to be carried out to determine whether the same proteins are present during DSB repair or whether new interactions are being made. Therefore protein purification assays should be carried out following incubation with the DSB-inducing agent 4NQO. To stabilise any interactions being made by Mre11-Rad50, crosslinking with EDC should also be implemented. Future work will hopefully uncover the structure and function of these proteins to elucidate how Mre11-Rad50 functions during DSB repair in *H. volcanii.*

References

Allers T, Barak S, Liddell S, Wardell K & Mevarech M. (2010) Improved strains and plasmid vectors for conditional overexpression of His- tagged proteins in Haloferax volcanii. Appl Environ Microbiol 76: 1759-1769.

Allers T, Mevarech M. (2005) Archaeal genetics - the third way. Nat Rev Genet 6: 58–73.

Allers T, Ngo HP, Mevarech M, & Lloyd RG. (2004) Development of additional selectable markers for the halophilic archaeon Haloferax volcanii based on the leuB and trpA genes. Appl Environ Microbiol 70: 943-953.

Andoh T, Ide T. (1972) Strand Scission and Rejoining of DNA in Cultured Mammalian Cells Induced by 4-Nitroquinoline 1-Oxide1. Cancer Res., 32, 1230–1235

Aravind L, Koonin EV. (2001) Prokaryotic homologs of the eukaryotic DNA-end-binding protein Ku, novel domains in the Ku protein and prediction of a prokaryotic double-strand break repair system. Genome Res;11:1365–1374.

Aravind L, Walker DR & Koonin, E.V. (1999) Conserved domains in DNA repair proteins and evolution of repair systems. *Nucleic Acids Res* **27:** 1223–1242.

Bab-Dinitz EH, Shmuely J, Maupin-Furlow J, Eichler & B. Shaanan. (2006) Haloferax volcanii PitA: an example of functional interaction between the Pfam chlorite dismutase and antibiotic biosynthesis monooxygenase families? Bioinformatics 22: 671-675.

Bassing CH, Swat W & Alt FW. (2002) The mechanism and regulation of chromosomal V(D)J recombination. Cell 109 Suppl: S45-55.

Bentchikou E, Servant P, Coste G, Sommer S. (2007) Additive effects of SbcCD and PolX deficiencies in the in vivo repair of DNA double-strand breaks in Deinococcus radiodurans. J Bacteriol. 189: 4784–4790.

Bill CA, Nickoloff JA. (2001) Ultraviolet light-induced and spontaneous recombination in eukaryotes: roles of DNA damage and DNA repair proteins. In: Nickoloff JA, Hoekstra MF, eds. DNA Damage and Repair, Advances from Phage to Humans. Totowa, NJ: Humana Press. pp 329–357.

Bischoff KM & Rodwell VW. (1996) 3-Hydroxy-3-methylglutaryl-coenzyme A reductase from Haloferax volcanii: purification, characterization, and expression in Escherichia coli. J Bacteriol 178: 19-23.

Bitan-Banin G, Ortenberg R &Mevarech M. (2003) Development of a gene knockout system for the halophilic archaeon Haloferax volcanii by use of the pyrE gene. J Bacteriol 185: 772-778.

Blecher O, Goldman S & Mevarech M. (1993) High expression in Escherichia coli of the gene coding for dihydrofolate reductase of the extremely halophilic archaebacterium Haloferax volcanii. Reconstitution of the active enzyme and mutation studies. Eur J Biochem 216: 199-203.

Blackwood JK, Rzechorzek NJ, Abrams AS, Maman JD, Pellegrini L et al. (2012) Structural and functional insights into DNA-end processing by the archaeal HerA helicase-NurA nuclease complex. Nucleic Acids Res 40: 3183- 3196.

Blackwood JK, Rzechorzek NJ, Bray SM, Maman JD, Pellegrini L et al. (2013) End-resection at DNA double-strand breaks in the three domains of life. Biochem Soc Trans 41: 314-320.

Bowater R & A. J. Doherty AJ (2006) Making ends meet: repairing breaks in bacterial DNA by non-homologous end-joining. PLoS Genet 2: e8.

Bressan DA, Baxter BK & Petrini JH. (1999) The Mre11-Rad50-Xrs2 protein complex facilitates homologous recombination-based double-strand break repair in Saccharomyces cerevisiae. Mol Cell Biol 19: 7681-7687.

Brissett NC & Doherty AJ. (2009 Repairing DNA double-strand breaks by the prokaryotic non-homologous end-joining pathway. Biochem Soc Trans 37: 539-545.

Brochier-Armanet C, Boussau B, Gribaldo S & Forterre P. (2008) Mesophilic crenarchaeota: proposal for a third archaeal phylum, the Thaumarchaeota. Nature Reviews Microbiology 6: 245-252.

Brochier-Armanet C, Forterre P & Gribaldo S. (2011) Phylogeny and evolution of the Archaea: one hundred genomes later. Current Opinion in Microbiology 14: 274-281.

Breuert S, Allers T, Spohn G & Soppa J. (2006) Regulated polyploidy in halophilic archaea. PLoS One 1: e92.

Buis J, Stoneham T, Spehalski E, Ferguson DO. (2012) Mre11 regulates CtIP-dependent double-strand break repair by interaction with CDK2. Nat. Struct. Mol. Biol. 2012;19:246–252.

Chapman JR, Taylor MR & Boulton SJ. (2012) Playing the end game: DNA double-strand break repair pathway choice. Mol Cell. 47: 497-510.

Christian JH & Waltho JA. (1962) Solute concentrations within cells of halophilic and non-halophilic bacteria. Biochim Biophys Acta. 65: 506-508.

Cline SW, Schalkwyk LC & Doolittle WF. (1989) Transformation of the archaebacterium Halobacterium volcanii with genomic DNA. J Bacteriol 171: 4987-4991.

Connaris H, Chaudhuri JB, Danson MJ & Hough DW. (1999) Expression, reactivation, and purification of enzymes from Haloferax volcanii in Escherichia coli. Biotechnology and bioengineering. 64: 38-45.

Connelly JC & Leach DR. (2002) Tethering on the brink: the evolutionarily conserved Mre11-Rad50 complex. Trends Biochem Sci 27: 410–418.

Constantinesco F, Forterre P & Elie C. (2002) NurA, a novel 5'-3' nuclease gene linked to rad50 and mre11 homologs of thermophilic Archaea. EMBO Rep 3: 537-542.

Constantinesco F, Forterre P, Koonin EV, Aravind L & Elie C. (2004) A bipolar DNA helicase gene, herA, clusters with rad50, mre11 and nurA genes in thermophilic archaea. Nucleic Acids Res 32: 1439-1447.

Cummings L J, Snyder MA & Brisack K (2009) Protein chromatography on hydroxyapatite columns. Methods Enzymol 463: 387-404.

De Jager M, Van Noort J, Van Gent DC, Dekker C, Kanaar R et al. (2001) Human Rad50/Mre11 is a flexible complex that can tether DNA ends. Mol Cell 8: 1129-1135.

Delmas S, Duggin IG &Allers T. (2013) DNA damage induces nucleoid compaction via the Mre11-Rad50 complex in the archaeon Haloferax volcanii. Mol Microbiol. 87: 168-179.

Delmas S, Shunburne L, Ngo HP & Allers Y. (2009) Mre11-Rad50 promotes rapid repair of DNA damage in the polyploid archaeon Haloferax volcanii by restraining homologous recombination. PLoS genetics 5: e1000552.

Game JC, Mortimer RK. (1974) A genetic study of x-ray sensitive mutants in yeast. Mutat Res 24: 281–292.

Giroux X, MacNeill SA. (2015) A novel archaeal DNA repair factor that acts with the UvrABC system to repair mitomycin C-induced DNA damage in a PCNA-dependent manner. Molecular Microbiology 10.1111/mmi.13210

Glickman B, Van Den Elsen P & Radman M. (1978) Induced mutagenesis in dam-mutants of Escherichia coli: a role for 6-methyladenine residues in mutation avoidance. Mol Gen Genet 163: 307-312.

Goosen N & Moolenaar GF (2008) Repair of UV damage in bacteria. DNA Repair (Amst) 7: 353-379.

Graham WJT, Rolfsmeier ML & Haseltine CA. (2013) An archaeal RadA paralog influences presynaptic filament formation. DNA Repair (Amst) 12: 403-413.

Haldenby ST. (2007) Genetic analysis of RadB, a paralogue of the archaeal Rad51/RecA homologue, RadA. University of Nottingham.

Hawkins M, Malla S, Blythe MJ, Nieduszynski CA, Allers T. (2013). Accelerated growth in the absence of DNA replication origins. Nature 503 544–547 10.1038/nature12650

Hohn MJ, Hedlund BP & Huber H (2002) Detection of 16S rDNA sequences representing the novel phylum "Nanoarchaeota": Indication for a wide distribution in high temperature biotopes. Systematic and Applied Microbiology. 25: 551-554.

Holmes ML, Nuttall SD & Dyall-Smith ML. (1991) Construction and use of halobacterial shuttle vectors and further studies on Haloferax DNA gyrase. J Bacteriol 173: 3807-3813.

Holthausen JT, Van Loenhout MT, Sanchez H, Ristic D, Van Rossum-Fikkert SE et al. (2011) Effect of the BRCA2 CTRD domain on RAD51 filaments analyzed by an ensemble of single molecule techniques. Nucleic acids research 39: 6558-6567.

Hopfner KP, Craig L, Moncalian G, Zinkel RA, Usui T et al. (2002) The Rad50 zinc-hook is a structure joining Mre11 complexes in DNA recombination and repair. Nature 418: 562-566.

Hopkins BB & Paull TT. (2008) The P. furiosus mre11/rad50 complex promotes 5' strand resection at a DNA double-strand break. Cell 135: 250-260.

Howley PM, Israel MA, Law MF & Martin MA. (1979) A rapid method for detecting and mapping homology between heterologous DNAs. Evaluation of polyomavirus genomes. J Biol Chem 254: 4876-4883.

Huang Q, Liu L, Liu J, Ni J, She Q. & Shen, Y. (2015) Efficient 5'-3' DNA end resection by HerA and NurA is essential for cell viability in the crenarchaeon *Sulfolobus islandicus*. BMC Molecular Biology 2015, 16:2

Humbard MA, Zhou G & Maupin-Furlow JA. (2009) The N-terminal penultimate residue of 20S proteasome alpha1 influences its N(alpha) acetylation and protein levels as well as growth rate and stress responses of Haloferax volcanii. J Bacteriol 191: 3794-3803.

Ito K & Akiyama Y. (2005) Cellular functions, mechanism of action, and regulation of FtsH protease. Annu Rev Microbiol 59: 211-231.

Jager A, Samorski R, Pfeifer F & Klug G. (2002) Individual gvp transcript segments in *Haloferax mediterra- nei* exhibit varying half-lives, which are differentially affected by salt concentration and growth phase. *Nucleic Acids Res* **30:** 5436–5443.

Jolley KA, Rapaport E, Hough DW, Danson MJ, Woods WG et al. (1996) Dihydrolipoamide dehydrogenase from the halophilic archaeon Haloferax volcanii: homologous overexpression of the cloned gene. J Bacteriol 178: 3044-3048.

Keeney S. (2008) Spo11 and the Formation of DNA Double-Strand Breaks in Meiosis. Genome Dyn Stab 2: 81-123.

Kish A & DiRuggiero J. (2008) Rad50 is not essential for the Mre11-dependent repair of DNA double-strand breaks in Halobacterium sp. strain NRC-1. J Bacteriol 190: 5210–5216.

Kobayashi J, Antoccia A, Tauchi H, Matsuura S & Komatsu K. (2004) NBS1 and its functional role in the DNA damage response. DNA Repair (Amst) 3: 855-861.

Kobayashi J, Tauchi H, Sakamoto S, Nakamura A, Morishima K et al. (2002) NBS1 localizes to gamma-H2AX foci through interaction with the FHA/BRCT domain. Curr Biol 12: 1846-1851.

Kowalczykowski SC, Dixon DA, Eggleston AK, Lauder SD, Rehrauer WM. (1994) Biochemistry of homologous recombination in Escherichia coli. Microbiol Rev. 58:401–465.

Krejci L, Altmannova V, Spirek M & Zhao X (2012) Homologous recombination and its regulation. Nucleic Acids Res 40: 5795-5818.

Krishna S, Wagener BM, Liu HP, Lo Y-C, Sterk R, et al.4(2007) Mre11 and Ku regulation of double-strand break repair by gene conversion and break-induced replication. DNA Repair 6: 797–808.

Kuwabara N, Murayama Y, Hashimoto H, Kokabu Y, Ikeguchi M et al. (2012) Mechanistic insights into the activation of Rad51-mediated strand exchange from the structure of a recombination activator, the Swi5-Sfr1 complex. Structure 20: 440-449.

Lankinen MH, Vilpo LM & Vilpo JA. (1996) UV- and gamma-irradiation- induced DNA single-strand breaks and their repair in human blood granulocytes and lymphocytes. Mutat Res 352: 31-38.

Large A, Stamme C, Lange C, Duan Z, Allers T et al. (2007) Characterization of a tightly controlled promoter of the halophilic archaeon Haloferax volcanii and its use in the analysis of the essential cct1 gene. Mol Microbiol 66: 1092- 1106.

Lisby M, Barlow JH, Burgess RC & Rothstein R. (2004) Choreography of the DNA damage response: spa-tiotemporal relationships among checkpoint and repair proteins. Cell 118: 699–713.

Lee KY, Im J-S, Shibata E, Park J, Handa N, Kowalczykowski SC & Dutta A. (2015) MCM8-9 complex promotes resection of double-strand break ends by MRE11-RAD50-NBS1 complex. Nature Communications 7744 doi:10.1038/ncomms8744

Lee JH & Paull TT. (2005) ATM activation by DNA double-strand breaks through the Mre11-Rad50-Nbs1 complex. Science 308: 551–554.

Lengsfeld BM, Rattray AJ, Bhaskara V, Ghirlando R & Paull TT. (2007) Sae2 is an endonuclease that processes hairpin DNA cooperatively with the Mre11/Rad50/Xrs2 complex. *Mol. Cell* **28**, 638–651

Lestini R, Duan Z & Allers T. (2010) The archaeal Xpf/Mus81/FANCM homolog Hef and the Holliday junction resolvase Hjc define alternative pathways that are essential for cell viability in Haloferax volcanii. DNA repair 9: 994-1002.

Lewis LK, Storici F, Van Komen S, Calero S, Sung P, et al. (2004) Role of the nuclease activity of Saccharomyces cerevisiae Mre11 in repair of DNA double-strand breaks in mitotic cells. Genetics 166: 1701–1713.

LI GM. (2008) Mechanisms and functions of DNA mismatch repair. Cell Res 18: 85-98.

Lieber MR. (2010) The mechanism of double-strand DNA break repair by the nonhomologous DNA end-joining pathway. Annu Rev Biochem 79: 181-211.

Lio YC, Mazin AV, Kowalczykowski SC & Chen DJ (2003) Complex formation by the human Rad51B and Rad51C DNA repair proteins and their activities in vitro. J Biol Chem 278: 2469-2478

Liu J, Doty T, Gibson B & Heyer WD. (2010) Human BRCA2 protein promotes RAD51 filament formation on RPA-covered single-stranded DNA. Nat Struct Mol Biol 17: 1260-1262.

Lloyd RG, Buckman C. (1985) Identification and genetic analysis of sbcC mutations in commonly used recBC sbcB strains of Escherichia coli K-12. J Bacteriol 164: 836–844.

Luo G. et al. (1999) Disruption of mRad50 causes embryonic stem cell lethality, abnormal embryonic development, and sensitivity to ionizing radiation. Proc. Natl Acad. Sci. USA, 96, 7376–7381.

Ma JL, Kim EM, Haber JE & Lee SE. (2003) Yeast Mre11 and Rad1 proteins define a Ku-independent mechanism to repair double-strand breaks lacking overlapping end sequences. Mol Cell Biol 23: 8820-8828.

Mascarenhas J, Sanchez H, Tadesse S, Kidane D, Krishnamurthy M, et al. (2006) Bacillus subtilis SbcC protein plays an important role in DNA inter-strand cross-link repair. BMC Mol Biol 7: 20.

Mazin AV, Alexeev AA & Kowalczykowski SC. (2003) A novel function of Rad54 protein. Stabilization of the Rad51 nucleoprotein filament. J Biol Chem 278: 14029-14036.

Mazón G, Mimitou EP & Symington LS. (2010) SnapShot: Homologous Recombination in DNA Double-Strand Break Repair. Cell 142 DOI 10.1016/j.cell.2010.08.006.

McEntee K, Weinstock GM & Lehman IR. (1979) Initiation of general recombination catalyzed in vitro by the recA protein of Escherichia coli. Proc Natl Acad Sci U S A 76: 2615-2619.

McRobbie AM, Carter LG, Kerou M, Liu H, McMahon SA et al. (2009) Structural and functional characterisation of a conserved archaeal RadA paralog with antirecombinase activity. J Mol Biol 389: 661-673.

McVey M & Lee SE. (2008) MMEJ repair of double-strand breaks (director's cut): deleted sequences and alternative endings. Trends Genet 24: 529-538.

Meyer H & Popp O. (2008) Role(s) of Cdc48/p97 in mitosis. Biochem Soc Trans 36: 126-130.

Mimitou EP & Symington LS. (2008) Sae2, Exo1 and Sgs1 collaborate in DNA double-strand break processing. Nature 455: 770-774.

Moreno-Herrero F, De Jager M, Dekker NH, Kanaar R, Wyman C & Dekker C. (2005) Mesoscale conforma- tional changes in the DNA-repair complex Rad50/Mre11/ Nbs1 upon binding DNA. Nature 437: 440–443.

Mullakhanbhai MF & Larsen H. (1975) Halobacterium volcanii spec. nov., a Dead Sea halobacterium with a moderate salt requirement. Arch Microbiol 104: 207-214.

Nunoura T, Takaki Y, Kakuta J, Nishi S, Sugahara J et al. (2011) Insights into the evolution of Archaea and eukaryotic protein modifier systems revealed by the genome of a novel archaeal group. Nucleic Acids Research 39: 3204-3223.

Oren A. (1999) Bioenergetic aspects of halophilism. Microbiology and molecular biology reviews : MMBR 63: 334-348.

Orr-Weaver TL, Szostak JW, Rothstein RJ. (1981) Yeast transformation: a model system for the study of recombination. Proc Natl Acad Sci U S A 78: 6354–6358.

Paull TT & Gellert M. (1998) The 3' to 5' exonuclease activity of Mre11 facilitates repair of DNA double-strand breaks. Mol Cell 1: 969-979.

Paull TT & Gellert. (2000) A mechanistic basis for Mre11-directed DNA joining at microhomologies. PNAS 97: 6409-6414.

Raymann K., Forterre P, Brochier-Armanet C, Gribaldo S. (2014) Global phylogenomic analysis disentangles the complex evolutionary history of DNA replication in archaea. Genome Biol. Evol. 6, 192–212. 10.1093/gbe/evu004

Robison JG, Elliott J, Dixon K, Oakley GG. (2004) Replication protein A and the Mre11.Rad50.Nbs1 complex co-localize and interact at sites of stalled replication forks. J Biol Chem.;279(33):34802–34810

Sakai A & Cox MM. (2009) RecFOR and RecOR as distinct RecA loading pathways. J Biol Chem 284: 3264-3272.

Sanger F, Nicklen S & Coulson AR. (1977). DNA sequencing with chain-terminating inhibitors. Proc. Natl. Acad. Sci. 74: 5463-5467.

Schwartz EK & Heyer WD. (2011) Processing of joint molecule intermediates by structure-selective endonucleases during homologous recombination in eukaryotes. Chromosoma 120: 109-127.

Shrivastav M, De Haro LP & Nickoloff JA. (2008) Regulation of DNA double-strand break repair pathway choice. Cell Res 18: 134-147.

Sigurdsson S, Van Komen S, Bussen W, Schild D, Albala JS et al. (2001) Mediator function of the human Rad51B-Rad51C complex in Rad51/RPA- catalyzed DNA strand exchange. Genes Dev 15: 3308-3318.

Sinha RP & Hader DP. (2002) UV-induced DNA damage and repair: a review. Photochem Photobiol Sci. 1: 225-236.

Sleytr UB & Messner P. (1983) Crystalline surface layers on bacteria. Annu Rev Microbiol 37: 311-339.

Sonoda E, Hochegger H, Saberi A, Taniguchi Y, Takeda S. (2006) Differential usage of non-homologous end-joining and homologous recombination in double strand break repair. DNA Repair (Amst) 5: 1021–1029.

Stewart GS et al. (1999) The DNA double-strand break repair gene hMRE11 is mutated in individuals with an ataxia-telangiectasia-like disorder. Cell 99: 577–587

Stracker TH & Petrini JH. (2011) The MRE11 complex: starting from the ends. Nat Rev Mol Cell Biol 12: 90-103.

Stroud A, Liddell S &Allers T. (2012) Genetic and Biochemical Identification of a Novel Single-Stranded DNA-Binding Complex in Haloferax volcanii. Frontiers in microbiology 3: 224.

Sugiyama T & Kowalczykowski SC (2002) Rad52 protein associates with replication protein A (RPA)-single-stranded DNA to accelerate Rad51- mediated displacement of RPA and presynaptic complex formation. J Biol Chem 277: 31663-31672.

Sung P. (1997) Yeast Rad55 and Rad57 proteins form a heterodimer that functions with replication protein A to promote DNA strand exchange by Rad51 recombinase. Genes & development 11: 1111-1121.

Symington LS & Gautier J. (2011) Double-strand break end resection and repair pathway choice. Annu Rev Genet 45: 247-271.

Takata M, Sasaki MS, Sonoda E, Morrison C, Hashimoto M et al. (1998) Homologous recombination and non-homologous end-joining pathways of DNA double-strand break repair have overlapping roles in the maintenance of chromosomal integrity in vertebrate cells. EMBO J 17: 5497–5508.

Tittel-Elmer M, Alabert C, Pasero P, J.A. Cobb (2009) The MRX complex stabilizes the replisome independently of the S phase checkpoint during replication stress. EMBO J., 28 pp. 1142–1156

Trujillo KM, Yuan S-S, Lee EY, Sung P. (1998) Nuclease activities in a complex of human recombination and DNA repair factors Rad50, Mre11, and p95. J. Biol. Chem. 273:21447–21450.

Quaiser A, Constantinesco F, White MF, Forterre P, Elie C. (2008) The Mre11 protein interacts with both Rad50 and the HerA bipolar helicase and is recruited to DNA following gamma irradiation in the archaeon Sulfolobus acidocaldarius. BMC Mol Biol;9:25.

Usui T et al. (1998) Complex formation and functional versatility of Mre11 of budding yeast in recombination. Cell 95:705–716.

Walker JR, Corpina RA & Goldberg J. (2001) Structure of the Ku heterodimer bound to DNA and its implications for double-strand break repair. Nature 412: 607-614.

Wardell, K. (2013) Regulation of Homologous Recombination in the Archaeon Haloferax volcanii. University of Nottingham.

Weller GR & Doherty AJ. (2001) A family of DNA repair ligases in bacteria? FEBS Lett 505: 340-342.

Wendoloski D, Ferrer C & Dyall-Smith ML. (2001) A new simvastatin (mevinolin)-resistance marker from Haloarcula hispanica and a new Haloferax volcanii strain cured of plasmid pHV2. Microbiology 147: 959-964.

West SC. (2003) Molecular views of recombination proteins and their control. Nat Rev Mol Cell Biol 4: 435-445.

Wigley DB. (2013) Bacterial DNA repair: recent insights into the mechanism of RecBCD, AddAB and AdnAB. Nat Rev Microbiol 11: 9-13.

Williams RS, Moncalian G, Williams JS, Yamada Y, Limbo O, Shin DS et al. (2008) Mre11 dimers coordi- nate DNA end bridging and nuclease processing in double-strand-break repair. Cell 135: 97–109.

Winker S & Woese CR. (1991) A definition of the domains Archaea, Bacteria and Eucarya in terms of small subunit ribosomal RNA characteristics. Syst Appl Microbiol 14: 305-310.

Winter JA, Patoli B & Bunting KA. (2012) DNA binding in high salt: analysing the salt dependence of replication protein A3 from the halophile Haloferax volcanii. Archaea 2012: 719092.

Woese CR & Fox GE. (1977) Phylogenetic structure of the prokaryotic domain: the primary kingdoms. Proc Natl Acad Sci U S A 74: 5088-5090.

Woese CR, Kandler O &Wheelis ML. (1990) Towards a natural system of organisms: proposal for the domains Archaea, Bacteria, and Eucarya. Proc Natl Acad Sci U S A 87: 4576-4579.

Zahradka K, Slade D, Bailone A, Sommer S, Averbeck D, et al. (2006) Reassembly of shattered chromosomes in Deinococcus radiodurans. Nature 443: 569–573

Zhang Y, Hefferin ML, Chen L, Shim EY, Tseng HM et al. (2007) Role of Dnl4-Lif1 in non-homologous end-joining repair complex assembly and suppression of homologous recombination. Nat Struct Mol Biol.

Zhang S, Wei T, Hou G, Zhang C, Liang P, Ni J, Sheng D, Shen Y. (2008) Archaeal DNA helicase HerA interacts with Mre11 homologue and unwinds blunt-ended double-stranded DNA and recombination intermediates. DNA Repair (Amst);7:380–391.

Appendix: Mass Spectrometry Results

Mass Spectrometry results from His_6/StrepII-tagged Mre11-Rad50

Mre11: DNA double-strand break repair Nuclease

Postulated Mre11, MSMS data confirms this protein identity as Mre11

Source: SWISSPROT

Mass: 48146 **Score:** 223 **Matches:** 16(7) **Sequences:** 5(2)

DNA double-strand break repair protein Mre11

Query	Observed	Mr(expt)	Mr(calc)	Delta	Miss	Score	Expect	Rank	Unique	Peptide
18	811.3659	810.3586	810.3396	0.0191	0	21	16	1	U	R.DSSLGDFA.-
24	846.9086	1691.8026	1691.8036	-0.0010	0	76	5.2e-05	1	U	R.EMGLSSAALDVDETVR.A 25 26 27 28
29	849.3563	1696.6980	1696.7217	-0.0236	0	32	1.3	1	U	R.DELDYQFDPVDADR.A 30 31
34	854.9178	1707.8210	1707.8468	-0.0258	0	40	0.22	1	U	R.GYNLVEFTPDAVDIR.R 32 33 35
37	17.4459	1832.8772	1832.8792	-0.0020	0	57	0.0042	1	U	R.VESLLSDDPDAFVAAER.E 38 39

MASCOT Search Results

DNA double-strand break repair protein Mre11

Database: SwissProt

Score: 223

Nominal mass (M_r): 48146

Calculated pI: 4.20

Taxonomy: Haloferax volcanii DS2

Sequence similarity is available as an NCBI BLAST search of MRE11_HALVD against nr

Protein sequence coverage: 15%

Matched peptides shown in ***bold red***.

```
  1 MTRVIHTGDT HLGYQQYHSP ERRQDFLDAF ERVVADALDG DVDAVVHAGD
 51 LYHDRRPELP DLLGTLAALR RLDDAGIPFL AIVGNHESTR GGQWLDLFER
101 LGLATRLGRD PHVVGGVAFY GLDHVPRSRR DELDYQFDPV DADRAVLVAH
151 GLFTPFAHAD WETETVLAES NVDFDAVLLG DNHVPDTAEL DGTWVTYCGS
201 TERASASERD PRGYNLVEFT PDAVDIRRRT LETRPFAFVE VDLAGDEGIE
251 RVRQRVREFD LEDAVVIVEL RGEGETVTPA AVESFAVEEG ALVARVNDKR
301 DIDDDGDLAT DVTFADPDDA VRERVREMGL SSAALDVDET VRASKVADSN
351 VRDEVRERVE SLLSDDPDAF VAAERESDAE AEESESVEDA ADGEDAAAVE
401 DTAETAAEAA TDTDTETTAD TDSETAADPA ASRDSSLGDF A
```

Rad50: DNA double-strand break repair ATPase

Putative Rad50, MSMS data confirms this protein identity as Rad50

Source: SWISSPROT

Mass: 100028 **Score:** 514 **Matches:** 49(9) **Sequences:** 13(4) **emPAI:** 0.16

Query	Observed	Mr(expt)	Mr(calc)	Delta	Miss	Score	Expect	Rank	Unique	Peptide
52	454.2321	906.4496	906.4559	-0.0062	0	11	2.9e+02	1	U	K.NAAAYLER.V 53
55	459.7502	917.4858	917.4818	0.0040	0	44	0.16	1	U	R.VESLVDTR.A
57	466.2474	930.4802	930.4770	0.0032	0	45	0.13	1	U	R.ETLAEVNR.E 58 59 60
63	474.2291	946.4436	946.4356	0.0081	0	41	0.3	1	U	R.SALDDAEAR.F 61 64
71	500.2887	998.5628	998.5509	0.0120	0	30	3.1	1	U	K.LINATPSQR.Q 67 68 69 70
73	553.7715	1105.5284	1105.5251	0.0033	0	22	20	1	U	R.ESLESAVESR.S
80	575.7838	1149.5530	1149.5414	0.0116	0	56	0.0078	1	U	R.AQAFETQAER.L 74 75 76 77 78 79
82	595.2896	1188.5646	1188.5622	0.0024	0	49	0.044	1	U	R.EAAVESLEADR.E 83 84 85
86	625.3144	1248.6142	1248.6085	0.0058	0	23	14	2	U	R.ESLAETETELK.N 87 89
91	638.8020	1275.5894	1275.5830	0.0064	0	102	2e-07	1	U	R.ETVDEEAVEGAK.Q 92 93 94 95 96 97
104	696.3174	1390.6202	1390.6099	0.0103	0	52	0.018	1	U	R.EAAAELDSEAEEK.R 102 103 105 106 107 108
112	779.8760	1557.7374	1557.7271	0.0104	0	21	21	1	U	K.DGTALEPEQLSGGER.A 111 113 114
115	781.3600	1560.7054	1560.6903	0.0151	0	23	11	1	U	R.EAAEVDAETAAEAER.E

MASCOT Search Results

DNA double-strand break repair Rad50 ATPase

Database: SwissProt

Score: 514

Nominal mass (M_r): 100028

Calculated pI: 4.48

Taxonomy: Haloferax volcanii DS2

Sequence similarity is available as an NCBI BLAST search of RAD50_HALVD against nr.

Protein sequence coverage: 15%

Matched peptides shown in ***bold red***.

```
  1 MRFTRIAIRN FKPYEDAELD LRDGVTVIHG VNGSGKSSLL EACFFALYGS
 51 KALAGTLEDV VTTGADDAEI TLEFVHDGGE YRIDRRVRVS GDRATTAKCV
101 LDGPEGTVEG ARDVRRHVAS LLRMDAEAFV NCAYVQQGEV NKLINATPSQ
151 RQDMIDDLLQ LGKLETYRER AGNARLGVED VLTKKRSVLE DVESQIEAKE
201 DADLHATLNA LESELDSLDE EISNYESQRD KAKSALDAAE ATLDEHAEKR
251 ERLDEIESAI EDLTAKISAD ETKRDDLSER VRELDAAADE LESDIDDALA
301 RADLDDASDE AIADAREALS ARESELRDDL SEARTRAQAF ETQAERLRER
351 ADDLESRAEE KREAAEVDAE TAAEAERELE SFRETRAELR SALDDAEARF
401 EDAPVELGEA ADLLEERREA RSEARESLAE TETELKNARE RLAEAERLRD
451 AGKCPECGQP VEGSPHVDAI SEREAAVESL EADRESLESA VESRSAAVEA
501 AEALVEVETR ASSRRDRLDL VDERIADREE TVESRREAAE EKREAAAELD
551 SEAEEKREAA TTQAERAEEV AETVDSLESD LDTLDDRRDR LDRVESLVDT
601 RAEKIDARDR LREKRETLAE VNRERREHLR ERRERRDELR ETVDEEAVEG
651 AKQRKKNAAA YLERVEDEVL PELREKRDDL QSRVGGVEAE LEQLDDLRER
701 RDHLAERVDA LESVHDEVST LESTYGDLRA ELRQRNVEVL ERMLNETFDL
751 VYANDAYSRI RLDGEYGLTV FQKDGTALEP EQLSGGERAL FNLSLRCAIY
801 RLLAEGIDGA APLPPLILDE PTVFLDGGHV SRLVDLVEDM QSRGVKQILI
851 VSHDEDLVGA ADDLVRVEKN PTTNRSTVER TDAPIVEGAL ADD
```

Mre11-Rad50 protein partners

A number of proteins were identified by mass spectrometry which purified with Mre11-Rad50 in *H. volcanii* from the His_6/StrepII columns. Among these were the recombination mediator RadA, which has not been previously seen to be interacting with Mre11-Rad50. HVO 1620 (XerC/D-like integrase) was also identified, which is thought to be a functional partner of Rad50. Also included are the proteins found with the highest number of matches. Numerous other proteins were found, however further mass spectrometry needs to be performed to verify their identity.

Sources: Swissprot and Mascot

HVO_0104|radA|gene
Mass: 37298 **Score:** 252 **Matches:** 7(7) **Sequences:** 4(4) **emPAI:** 0.47

radA | product DNA repair and recombination protein RadA | note DNA metabolism

Query	Observed	Mr(expt)	Mr(calc)	Delta	Miss	Score	Expect	Rank	Unique	Peptide
558	518.2710	1034.5275	1034.5284	-0.0009	0	44	0.00073	1	U	K.ALVDDFLDK.I
950	800.9043	1599.7940	1599.7926	0.0013	0	76	3.2e-007	1	U	R.LVDAPNLADGEAIMR.V 949
981	885.4046	1768.7947	1768.7938	0.0009	0	78	2.4e-007	1	U	R.DAADVGGFETGSMVLER.R
985	892.9309	1783.8473	1783.8476	-0.0003	0	58	2.2e-005	1	U	M.AEDDLESLPGVGPATADK.L 984 986

HVO_1620|-|product
Mass: 39084 **Score:** 252 **Matches:** 6(5) **Sequences:** 4(3) **emPAI:** 0.44

XerC/D-like integrase | note DNA metabolism

Query	Observed	Mr(expt)	Mr(calc)	Delta	Miss	Score	Expect	Rank	Unique	Peptide
592	613.2956	1224.5766	1224.5775	-0.0009	0	43	0.00053	1	U	R.AFESFLGDPSR.N
887	852.9179	1703.8213	1703.8214	-0.0001	0	74	4.5e-007	1	U	R.DVSLSAETPLDDVSTR.A 888
895	877.9806	1753.9467	1753.9462	0.0005	0	87	2e-008	1	U	R.STVVPVDDELEAVLLR.W 896
929	1053.0086	2104.0026	2104.0073	-0.0047	0	17	0.16	1	U	R.GPSIYVAADPSVGSVTNGEER.T

EF1A_HALWD
Mass: 45585 **Score:** 655 **Matches:** 35(14) **Sequences:** 7(5) **emPAI:** 1.79

Elongation factor 1-alpha OS=Haloquadratum walsbyi (strain DSM 16790 / HBSQ001) GN=tuf PE=3 SV=1

Query	Observed	Mr(expt)	Mr(calc)	Delta	Miss	Score	Expect	Rank	Unique	Peptide
1023	915.9409	1829.8673	1830.8523	-0.9851	0	43	0.17	1	U	K.LDPASGEVAEEDPDFIK.S 1018 1019 1020 1021 1022
1027	924.4182	1846.8219	1846.8196	0.0023	0	(47)	0.067	1	U	K.GGFEFAYVMDNLAEER.E
1029	932.4138	1862.8130	1862.8145	-0.0015	0	90	2.9e-006	1	U	K.GGFEFAYVMDNLAEER.E 1028
1046	993.0564	1984.0982	1984.0994	-0.0012	0	85	9.1e-006	1	U	R.LPIQDVYTISGIGTVPVGR.V 1047 1048
1049	662.3737	1984.0992	1984.0994	-0.0001	0	(51)	0.022	1	U	R.LPIQDVYTISGIGTVPVGR.V 1050
1054	664.3498	1990.0276	1990.0272	0.0003	0	58	0.0043	1	U	R.LLFETGSVPEHVIEQHR.E 1053 1055
1056	498.5142	1990.0276	1990.0272	0.0004	0	(39)	0.35	1	U	R.LLFETGSVPEHVIEQHR.E 1057 1058
1148	635.0423	2536.1401	2536.1401	-0.0000	0	(92)	1.4e-006	1	U	K.TVEMHHEEVDQAGPGDNVGFNVR.G 1146 1147
1151	846.3883	2536.1430	2536.1401	0.0029	0	94	8.2e-007	1	U	K.TVEMHHEEVDQAGPGDNVGFNVR.G 1149 1150
1203	895.4479	2683.3220	2683.3235	-0.0015	0	82	1.2e-005	1	U	K.NMITGASQADNAVLVVAADDGVAPQTR.E
1207	900.7788	2699.3145	2699.3185	-0.0040	0	(67)	0.00044	1	U	K.NMITGASQADNAVLVVAADDGVAPQTR.E 1206 1208
1212	677.3397	2705.3299	2705.3296	0.0003	1	31	1.7	1	U	R.LLFETGSVPEHVIEQHREEAEEK.G 1211 1214
1213	902.7840	2705.3302	2705.3296	0.0006	1	(31)	1.7	1	U	R.LLFETGSVPEHVIEQHREEAEEK.G 1215

HVO_0359|tef1a1|gene

Mass: 45731 **Score:** 2350 **Matches:** 59(52) **Sequences:** 12(12) **emPAI:** 3.82

tef1a1 | product translation elongation factor aEF-1 alpha subunit | note Protein synthesis | evidence JMF-ORF01614

Query	Observed	Mr(expt)	Mr(calc)	Delta	Miss	Score	Expect	Rank	Unique	Peptide
904	670.9109	1339.8073	1339.8075	-0.0002	0	82	5.5e-008	1	U	R.TLGIGELIIAVNK.M 900 901 902 903
1022	915.9409	1829.8673	1829.8683	-0.0010	0	115	3.7e-011	1	U	K.LDPASGEVAEENPDFIK.S 1018 1019 1020 1021 1023
1027	924.4182	1846.8219	1846.8196	0.0023	0	(47)	0.00019	1	U	K.GGFEFAYVMDNLAEER.E
1029	932.4138	1862.8130	1862.8145	-0.0015	0	90	8e-009	1	U	K.GGFEFAYVMDNLAEER.E 1028
1046	993.0564	1984.0982	1984.0994	-0.0012	0	85	2.5e-008	1	U	R.LPIQDVYTISGIGTVPVGR.I 1047 1048
1049	662.3737	1984.0992	1984.0994	-0.0001	0	(51)	6.2e-005	1	U	R.LPIQDVYTISGIGTVPVGR.I 1050
1054	664.3498	1990.0276	1990.0272	0.0003	0	58	1.2e-005	1	U	R.LLFETGSVPEHVIEQHR.E 1053 1055
1056	498.5142	1990.0276	1990.0272	0.0004	0	(39)	0.001	1	U	R.LLFETGSVPEHVIEQHR.E 1057 1058
1112	811.0391	2430.0956	2430.0975	-0.0019	0	81	4.7e-008	1	U	R.FNSDDATYVPISAFEGDNIAER.S 1116 1117
1115	1216.0554	2430.0962	2430.0975	-0.0013	0	(59)	7.6e-006	1	U	R.FNSDDATYVPISAFEGDNIAER.S 1111 1113 1114
1121	1230.5975	2459.1804	2459.1816	-0.0012	0	116	2.5e-011	1	U	R.IETGTLNPGDNVSFQPSDVGGEVK.T 1124 1125
1123	820.7341	2459.1806	2459.1816	-0.0011	0	(89)	1.3e-008	1	U	R.IETGTLNPGDNVSFQPSDVGGEVK.T 1120 1122
1148	635.0423	2536.1401	2536.1401	-0.0000	0	(92)	4.1e-009	1	U	K.TVEMHHEEVDQAGPGDNVGFNVR.G 1146 1147
1151	846.3883	2536.1430	2536.1401	0.0029	0	94	2.3e-009	1	U	K.TVEMHHEEVDQAGPGDNVGFNVR.G 1149 1150
1203	895.4479	2683.3220	2683.3235	-0.0015	0	82	3.6e-008	1	U	K.NMITGASQADNAVLVVAADDGVAPQTR.E
1207	900.7788	2699.3145	2699.3185	-0.0040	0	(67)	1.5e-006	1	U	K.NMITGASQADNAVLVVAADDGVAPQTR.E 1206 1208
1212	677.3397	2705.3299	2705.3296	0.0003	1	31	0.0053	1	U	R.LLFETGSVPEHVIEQHREEAEEK.G 1211 1214
1213	902.7840	2705.3302	2705.3296	0.0006	1	(31)	0.0054	1	U	R.LLFETGSVPEHVIEQHREEAEEK.G 1215
1258	838.7045	3350.7889	3349.7881	1.0007	0	32	0.0023	1	U	K.SGDAAIVTVRPQKPLSIEPSSEIPELGSFAVR.D 1255 1256 1257
1259	1131.8929	3392.6568	3392.6524	0.0044	0	53	2.4e-005	1	U	R.SDNTSWYDGDILLEALNNLPAPQPPTDAPLR.L 1260

HVO_2471|-|product

Mass: 56505 **Score:** 2942 **Matches:** 89(74) **Sequences:** 10(8) **emPAI:** 1.44

propionyl-CoA carboxylase complex B chain | note Fatty acid and phospholipid metabolism | evidence JMF-ORF02520 start site changed to match JMF

Query	Observed	Mr(expt)	Mr(calc)	Delta	Miss	Score	Expect	Rank	Unique	Peptide
734	651.7757	1301.5369	1301.5371	-0.0002	0	22	0.067	1	U	R.DELDAADDPDAR.R 735
765	665.8518	1329.6891	1329.6888	0.0003	0	21	0.1	1	U	R.VNAGTLNINASEK.G 764
813	681.3215	1360.6284	1360.6299	-0.0015	0	87	2.2e-008	1	U	R.IDYFLDDGTFR.E 810 811 812 814 815 816 817 818 819 820 821
884	724.3559	1446.6973	1446.6991	-0.0018	0	81	8.6e-008	1	U	R.GFIDDVIEPGETR.E 881 882 883 885 886 887 888 889 890 891 892
906	748.3722	1494.7299	1494.7315	-0.0015	0	51	7.9e-005	1	U	R.VDDDLAGVVPDQPR.K 902 903 904 905 907 908 909
918	773.8961	1545.7776	1545.7787	-0.0012	0	107	2e-010	1	U	K.LPGDGVITGYGEVGGR.T 917 919 920 921 922 923 924 925 926 928
930	520.9287	1559.7642	1559.7654	-0.0012	0	(31)	0.0075	1	U	R.DTSHMFITGPDVIK.T
931	780.8898	1559.7650	1559.7654	-0.0004	0	103	4.8e-010	1	U	R.DTSHMFITGPDVIK.T 932 933
934	788.8870	1575.7595	1575.7603	-0.0008	0	(103)	4.4e-010	1	U	R.DTSHMFITGPDVIK.T
935	526.2609	1575.7607	1575.7603	0.0004	0	(50)	9.2e-005	1	U	R.DTSHMFITGPDVIK.T
953	857.4330	1712.8515	1712.8516	-0.0001	0	92	6e-009	1	U	K.AMEVGAPVVGLNDSAGAR.I 951 952 954 955
959	865.4311	1728.8477	1728.8465	0.0013	0	(84)	3.9e-008	1	U	K.AMEVGAPVVGLNDSAGAR.I 960 961 962 963 964 965 966
968	868.9511	1735.8876	1735.8893	-0.0017	0	133	5.3e-013	1	U	R.IQEGVQSLGGFGEIFR.R 967 969 970 971 972
974	579.6372	1735.8899	1735.8893	0.0005	0	(62)	6.1e-006	1	U	R.IQEGVQSLGGFGEIFR.R
994	946.4859	1890.9572	1890.9588	-0.0016	0	(52)	5.7e-005	1	U	R.HLLSYLPQNNVEDPPR.V 993 995
997	631.3270	1890.9592	1890.9588	0.0004	0	60	8.3e-006	1	U	R.HLLSYLPQNNVEDPPR.V 996 998

HVO_2486|bccA|gene

Mass: 65306 **Score:** 2321 **Matches:** 62(57) **Sequences:** 12(10) **emPAI:** 0.84

pccA | product propionyl-CoA carboxylase biotin carboxylase component | note Fatty acid and phospholipid metabolism

Query	Observed	Mr(expt)	Mr(calc)	Delta	Miss	Score	Expect	Rank	Unique	Peptide
729	548.2784	1094.5422	1094.5430	-0.0008	0	66	3.1e-006	1	U	R.LMLTDEAFR.E 727 728 730
791	617.3272	1232.6398	1232.6401	-0.0003	0	52	7.3e-005	1	U	R.ALAEFDIEGLR.T 789 790
793	617.8003	1233.5861	1233.5877	-0.0017	0	44	0.00046	1	U	K.YLDEVLDPDR.I 794 795 796 797 798
886	670.3184	1338.6223	1338.6204	0.0019	0	12	0.66	1	U	R.YADEAYNIGPAR.A
947	690.3632	1378.7119	1378.7133	-0.0014	0	84	4.4e-008	1	U	K.AVADEFGYPVAIK.A 945 946 948 949 950 951 952 953 954 958
1004	806.4138	1610.8131	1610.8151	-0.0021	0	80	9.5e-008	1	U	K.VIEEAPSPALSDDLR.E 1005 1006 1007 1008 1009 1010 1011
1029	860.8898	1719.7651	1719.7628	0.0023	0	93	4.4e-009	1	U	R.EGEAYFDNASVYVEK.Y 1028 1030
1032	873.9181	1745.8217	1745.8220	-0.0003	0	79	1.2e-007	1	U	R.AADSYLDHESVIEAAR.K 1031
1053	1032.4178	2062.8211	2062.8240	-0.0028	0	120	8e-012	1	U	R.WSPEAVADDDDDDEVTER.T 1046 1047 1048 1049 1050 1051 1052
1056	1045.5302	2089.0459	2089.0480	-0.0021	0	66	2.1e-006	1	U	K.EFAPATGTLATYDPPGGIGVR.M 1057 1058
1064	728.6691	2182.9855	2182.9841	0.0014	1	12	0.64	1	U	R.KVEESEFTWVGPSADAMER.L
1098	1257.1068	2512.1991	2512.2003	-0.0012	0	(31)	0.0057	1	U	R.ALMQDADVPVVPGTTEPADSAADVK.A
1099	838.4076	2512.2010	2512.2003	0.0007	0	56	1.5e-005	1	U	R.ALMQDADVPVVPGTTEPADSAADVK.A 1100 1101

HVO_0481|gap|gene

Mass: 37633 **Score:** 421 **Matches:** 12(8) **Sequences:** 5(4) **emPAI:** 0.46

gap | product glyceraldehyde-3-phosphate dehydrogenase| type I | note Energy metabolism

Query	Observed	Mr(expt)	Mr(calc)	Delta	Miss	Score	Expect	Rank	Unique	Peptide
727	649.3212	1296.6278	1296.6285	-0.0007	0	34	0.0064	1	U	R.MLDVAHFVTHQ.-
920	740.4298	1478.8450	1478.8457	-0.0007	0	(10)	1.2	1	U	R.VPVPNGSLTELVVR.L 919 921 922
979	870.4082	1738.8018	1738.8010	0.0009	0	122	9.4e-012	1	U	K.SYLSAGENVDESDVVR.V 976 977 978
980	587.9598	1760.8574	1760.8581	-0.0006	0	84	4.6e-008	1	U	R.LEDKPSVEEINDAFR.A
983	889.4124	1776.8103	1776.8107	-0.0004	0	76	3.7e-007	1	U	K.ILTWYDNEYGFSNR.M 982